Measure of the density of quantum states in information geometry and quantum multiparameter estimation

Haijun Xing and Libin Fu*
Graduate School of China Academy of Engineering Physics, Beijing 100193, China

(Received 20 May 2020; revised 28 August 2020; accepted 3 December 2020; published 23 December 2020)

Recently, there is growing interest in studying quantum mechanics from the information geometry perspective, where a quantum state is depicted by a point in the projective Hilbert space (PHS). However, the absence of high-dimensional measures limits information geometry in the study of multiparameter systems. In this paper, we propose a measure of the intrinsic density of quantum states (IDQS) in the PHS with the volume element of quantum Fisher information (QFI). Theoretically, the IDQS is a measure to define the (over)completeness relation of a class of quantum states. As an application, the IDQS is used to study quantum measurement and multiparameter estimation. We find that the density of distinguishable states (DDS) for a set of efficient estimators is measured by the invariant volume element of the classical Fisher information, which is the classical counterpart of the QFI and serves as the metric of statistical manifolds. The ability to infer the IDQS via quantum measurement is studied with a determinant-form quantum Cramér-Rao inequality. As a result, we find a gap between the IDQS and the maximal DDS over the measurements. The gap has tight connections with the uncertainty relationship. Exemplified by the three-level system with two parameters, we find that the Berry curvature characterizes the square gap between the IDQS and the maximal attainable DDS. Specific to *vertex measurements*, the square gap is proportional to the square of the Berry curvature.

DOI: 10.1103/PhysRevA.102.062613

I. INTRODUCTION

Estimating parameters with a high precision is essential for both scientific research and technical applications. Recently, studies of estimating multiple parameters simultaneously using quantum resources have attracted lots of attention [1–13]. The theory of quantum parameter estimation [14,15] and quantum metrology [16–18] provides us the basic tools to estimate a single parameter via quantum measurement and methods of enhancing the precision of parameter estimation with quantum resources. Quantum Fisher information (QFI) lies at the heart of the theory by setting the upper bounds of a single estimator's precision via the quantum Cramér-Rao inequality. The single-parameter case is well studied, and series of achievements [19–21], such as high-precision magnetometry [22–24], atomic clocks [25–28], and gravitational wave detectors [29,30], have been demonstrated in principle or realized experimentally.

Information geometry presents us with a fundamental viewpoint to study single-parameter estimation with differential geometrical methods [31–40]. By taking QFI as the Riemannian metric of the embedding parameter spaces, estimating a small parameter is equivalent to distinguishing neighboring quantum states along the curve given by the shift of the parameter to be estimated [40]. QFI measures the square of the density of states distinguishable in the neighborhood of the given point (states) along the curve. The ease of distinguishing two states via parameter estimation is thus quantified by the statistical distance, i.e., length of the geodesic line given by QFI [39,40]. The QFI and statistical distance have tight connections with the measures widely used in quantifying the "distance" between quantum states, such as the Fubini-Study metric [41], quantum geometric tensor [35], Bures distance [40], and Kullback-Leibler divergence (relative entropy) [36]. Especially, in some theoretical studies [42–45], the QFI, also known as the Bures metric, is defined via the fidelity between two infinitesimally close states [46–48]. As a metric, QFI also depicts the square of the speed of the quantum state's "movement" with respect to the small shift of the intrinsic or external control parameter. It is also known as the fidelity susceptibility [49–53] in these scenarios. Therefore, in the framework of information geometry, researchers can unify topics in quantum mechanics with parameter estimation, such as the quantum phase transition [54–58], quantum non-Markovianity [59], quantum speed limit [60–64], optimal control [65–69], quantum algorithm [70–72], and even thermodynamics [66,73–78].

In general cases such as vector magnetic field estimation [7], optical imaging [4], and wave-function detection, one simultaneously estimates more than one parameter from a given quantum state. These demands encourage the flourishing studies of multiparameter estimation. For the d-dimensional *estimand* $\boldsymbol{\theta}$, i.e., parameters to be estimated, the uncertainty of the corresponding unbiased estimators is depicted by its $(d \times d)$–dimensional covariance matrix. One of the primary tasks is extracting a scalar measure from the covariance matrix to assess the quality (precision) of these estimators and finding the saturable bounds of the measure. The quadratic cost function is the conventional measure widely used in current studies.

*lbfu@gscaep.ac.cn

It is the weighted average of covariance matrix entries, by introduction of a $(d \times d)$–dimensional nonnegative definite real symmetric matrix $\boldsymbol{G}$ to weight the asymmetrical significance of the parameters [14,15]. The cost function is bounded by a Cramér-Rao-type bound [14] and Holevo Cramér-Rao bound [10,15]. Much has been achieved with these measures [1–6,9]. Two extreme conditions are well studied: (i) $\boldsymbol{G} = \boldsymbol{n}\boldsymbol{n}^T$ [9]—the cost function only counts the variance in a specific direction $\boldsymbol{n}$ in the parameter space and reduces to the variance of a single parameter via reparameterization; and (ii) $\boldsymbol{G}$ is identity[4,13]—the corresponding cost function is the trace of the covariance matrix.

Estimating a set of d independent parameters $\boldsymbol{\theta}$ of a given quantum state is equivalent to inferring the coordinates of a given point in d-dimensional parameter space. Hence the precision of the corresponding estimation highly relates to the geometrical properties of the neighborhoods of the given point $\boldsymbol{\theta}$. However, it is hard to interpret the general cost function and its bounds as geometrical measures of the parameter space straightforwardly. The tight connections between information geometry and parameter estimation are thus loose in current multiparameter studies. This increases the difficulty of generalizing results acquired in recent studies to other topics highly related to the statistical properties of multiparameter quantum systems.

Theoretically, manifolds of the quantum system called complex projective Hilbert spaces [36–38] are intrinsically multidimensional. In practical studies, most of the manifolds we encountered, such as the ground-state manifolds [79], quantum phase transition [80,81], response theory [82–84], and even thermodynamics [66,77,78,85,86], are generally multidimensional too. Accurate characterization of the neighborhood of a given point in multidimensional manifolds is thus vital to understanding and promoting these studies. Hence finding a measure of multiparameter estimation from the information geometrical perspective is an essential and significant topic for quantum information fields.

In this article, we study multiparameter estimation from the information geometry perspective. We find that, as a Riemannian metric equipped in the parameter space, QFI's volume element quantifies the *intrinsic density of quantum states* (IDQS), which is a natural generalization of the "line element" in single-parameter cases. The IDQS is the measure for defining the (over)completeness relation of a class of states which forms submanifolds of the projective Hilbert space. As its classical counterpart, the volume element of classical Fisher information provides us the *density of distinguishable states* (DDS) in the statistical manifold. The DDS measures the maximal density of states that can be distinguished in a single shot of the given measurement, when the quality of a set of estimators built on its results is quantified via the volume occupied by their "error ball." The IDQS bounds the DDS via the quantum Cramér-Rao inequality in determinant form. Differently from the single-parameter case, this bound is not always attainable. A gap between the IDQS and the maximal DDS achieved via quantum measurement is found. We study the three-level system as an example, which is the minimal system for study of the gap. As a result, a tight connection between the gap and the Berry curvature is found.

This article is organized as follows. In Sec. II, we review single-parameter estimation from the information geometry perspective. In Sec. III, the DDS and IDQS are introduced. In Sec. IV, the ability to infer the IDQS with quantum measurements is studied via the quantum Cramér-Rao inequality in the determinant form. As a result, a gap between the maximal DDS and the IDQS is found. In Sec. V, a three-level system for study of the gap is proposed, and the tight connection between the gap and the Berry curvature is shown. Finally, we summarize the article in Sec. VI.

II. REVIEW OF THE QUANTUM GEOMETRIC TENSOR AND PARAMETER ESTIMATION

A. Quantum geometric tensor

In quantum mechanics, one usually terms the state space of an $(n+1)$–level system an $(n+1)$–dimensional Hilbert space. However, an additional equivalence, $|\psi\rangle \sim c|\psi\rangle$, with $c \in \mathbb{C}\backslash\{0\}$, is assumed implicitly. It depicts the demands of normalization and the physical insight that two states different only in the global phases are indistinguishable. Under this equivalence, the actual state space we handle is the so-called projective Hilbert space $\mathbb{C}\mathbf{P}^n$ or its submanifold generally [36–38]. Therefore, one usually parameterizes quantum states with the model $\mathcal{M} = \{|\psi(\boldsymbol{\theta})\rangle\langle\psi(\boldsymbol{\theta})||\boldsymbol{\theta} \in \Theta\}$, which gives the real coordinate system $\boldsymbol{\theta} = (\theta^1, \theta^2, \dots, \theta^d)$, with $d \leqslant 2n$, of (the submanifold of) $\mathbb{C}\mathbf{P}^n$ effectively. The movement along the "radial direction" of state $|\psi(\boldsymbol{\theta})\rangle$ is null under this equivalence. Based on that, the intrinsic derivative is given by

$$\hat{\nabla}_\mu|\psi\rangle \equiv (\hat{\mathbb{1}} - |\psi\rangle\langle\psi|)\hat{\partial}_\mu|\psi\rangle, \tag{1}$$

with $\hat{\partial}_\mu \equiv \partial/\partial\theta^\mu$, and $|\psi\rangle \equiv |\psi(\boldsymbol{\theta})\rangle$ for succinctness. The normalization $\langle\psi|\psi\rangle = 1$ is assumed. The derivative is orthogonal to state $|\psi\rangle$ with $\langle\psi|\hat{\nabla}_\mu|\psi\rangle = 0$. In this form, the quantum geometric tensor $\mathcal{Q}$ is defined as a $(d \times d)$–dimensional matrix with the entries [35]

$$\mathcal{Q}_{\mu\nu} \equiv \langle\psi|\overleftarrow{\hat{\nabla}}_\mu\hat{\nabla}_\nu|\psi\rangle = g^F_{\mu\nu} + i\sigma_{\mu\nu}, \tag{2}$$

$1 \leqslant \mu, \nu \leqslant d$, where the antisymmetric entry $\sigma_{\mu\nu} \equiv i(\mathcal{Q}_{\nu\mu} - \mathcal{Q}_{\mu\nu})/2 = -\mathcal{B}_{\mu\nu}/2$ is proportional to the Berry curvature $\mathcal{B}_{\mu\nu}$; the symmetric part $\boldsymbol{g}^F$ with $d \times d$ entries

$$g^F_{\mu\nu} \equiv \tfrac{1}{2}\langle\psi|(\overleftarrow{\hat{\nabla}}_\mu\hat{\nabla}_\nu + \overleftarrow{\hat{\nabla}}_\nu\hat{\nabla}_\mu)|\psi\rangle \tag{3}$$

serves as the Riemannian metric of the projective Hilbert spaces when $\mathbb{C}\mathbf{P}^n$ is treated as a $2n$-dimensional real manifold. We denote $\boldsymbol{g}^F$ the *quantum Fisher metric* (QFM) in this article, as it is a quarter of the quantum Fisher information (QFI) $\boldsymbol{\mathcal{F}}$. The QFM defines the statistical distance with [39,40]

$$ds^2 \equiv g^F_{\mu\nu}\dot{\theta}^\mu\dot{\theta}^\nu dt^2 = g^F_{tt}dt^2, \tag{4}$$

where $\dot{\theta}^\mu = d\theta^\mu/dt$ is the derivative along the curve $\boldsymbol{\theta}(t)$, and the Einstein summation convention is assumed. The length of a curve acquired by integrating the element ds depicts the maximal number of states distinguishable along the curve. The corresponding distance measures the ease of distinguishing the quantum states via quantum parameter estimation.

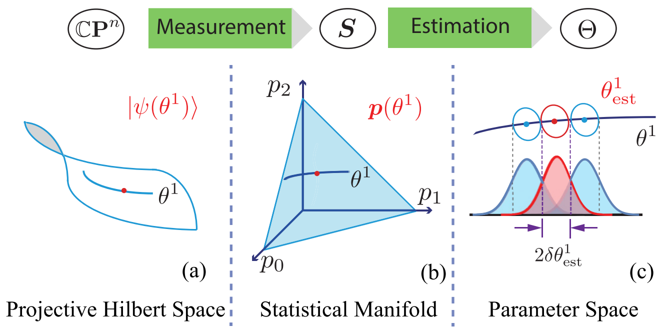

FIG. 1. Quantum single-parameter estimation (exemplified by the three-level system). (a) The state of the system located in the projective Hilbert space $\mathbb{C}\mathbf{P}^2$. Only one real parameter θ^1 is assumed to be unknown and requires estimation. State $|\psi(\theta^1)\rangle$ draws a curve in $\mathbb{C}\mathbf{P}^2$ via variation of θ^1. The statistical length of the curve is defined with the element $ds^2 = g^F_{11}(d\theta^1)^2$. (b) Via a ternary-outcome projective measurement $\{\hat{E}_i|i = 0, 1, 2\}$, state $|\psi(\theta^1)\rangle$ reduces to a classical distribution, $\boldsymbol{p}(\theta^1) = (p_0, p_1, p_2)$ with $p_i = \langle\psi(\theta^1)|\hat{E}_i|\psi(\theta^1)\rangle$. $\boldsymbol{p}(\theta^1)$ is located in a curve in the statistical manifold, which is a two-simplex. The density of the classical distribution along the curve is measured by $ds/d\theta^1 = \sqrt{g^I_{11}}$. The maximum of this density is $\sqrt{g^F_{11}}$, which can be reached via the optimal measurement. (c) One estimates the state, i.e., the parameter θ^1, with the sample acquired from a sequence of identical measurements. The width of the "error ball" of θ^1_{est} along the curve in the parameter space Θ is measured by $2\delta\theta^1_{\text{est}}$. Two distributions can be reliably distinguished when their error balls have no overlaps. If the estimation is efficient, the density of states distinguishable in a single shot of the given measurement is maximal, which equals $\sqrt{g^I_{11}}$.

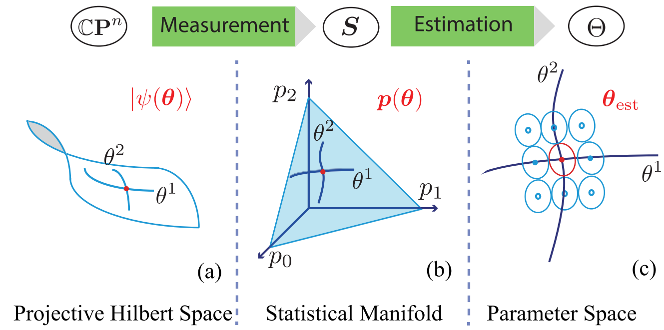

FIG. 2. Quantum multiparameter estimation (exemplified by the three-level system). (a) State $|\psi(\boldsymbol{\theta})\rangle$ of the system located in the projective Hilbert space $\mathbb{C}\mathbf{P}^2$. We focus on its two-dimensional submanifolds, where only two real parameters, $\boldsymbol{\theta} = \{\theta^1, \theta^2\}$, are assumed to be unknown and require estimation. The IDQS in this space is measured by $\mathcal{D}_Q(\boldsymbol{\theta})$. (b) Via a ternary-outcome projective measurement, $\{\hat{E}_i|i = 0, 1, 2\}$, state $|\psi(\boldsymbol{\theta})\rangle$ reduces to the classical distribution $\boldsymbol{p}(\boldsymbol{\theta}) = (p_0, p_1, p_2)$ with $p_i = \langle\psi(\boldsymbol{\theta})|\hat{E}_i|\psi(\boldsymbol{\theta})\rangle$. $\boldsymbol{p}(\boldsymbol{\theta})$ is located in a statistical manifold, which is a two-simplex. $\mathcal{D}_D(\boldsymbol{\theta})$ measures the DDS in this simplex. (c) One estimates the state, i.e., the parameters $\boldsymbol{\theta}$, with the sample acquired from a sequence of identical measurements. The volume occupied by the "error ball" of $\boldsymbol{\theta}_{\text{est}}$ in the parameter space Θ is measured by $\sqrt{|4\boldsymbol{\Sigma}|}$. Two distributions can be reliably distinguished when their error balls have no overlaps. The density of states distinguishable in a single shot of the given measurement is maximal for efficient estimation, which equals the DDS $\mathcal{D}_D(\boldsymbol{\theta})$.

B. Single-parameter estimation

In the process of parameter estimation as shown by Fig. 1 and 2, state $|\psi(\boldsymbol{\theta})\rangle$ is inferred via a set of positive operator-valued measurements (POVMs) $\hat{\boldsymbol{E}} = \{\hat{E}_i\}$ with $\sum_i \hat{E}_i = \hat{\mathbb{1}}$. The result i is acquired with probability $p_i = \langle\psi(\boldsymbol{\theta})|\hat{E}_i|\psi(\boldsymbol{\theta})\rangle$. Mathematically, the measurement reduces the projective Hilbert spaces of states $|\psi(\boldsymbol{\theta})\rangle$ to a statistical manifold of classical distribution $\boldsymbol{p} = (p_0, p_1, \ldots, p_n)$. Corresponding to the QFM, the metric of the statistical manifold is the *Fisher-Rao metric* (FRM) $\boldsymbol{g}^I$ with the $d \times d$ entries

$$g^I_{\mu\nu} \equiv \sum_i \partial_\mu\sqrt{p_i}\partial_\nu\sqrt{p_i}, \tag{5}$$

$1 \leqslant \mu, \nu \leqslant d$. The FRM is a quarter of the classical Fisher information (CFI) $\boldsymbol{\mathcal{I}}$. One builds estimators $\boldsymbol{\theta}_{\text{est}}$ of the parameters $\boldsymbol{\theta}$ with the sample acquired by the measurement results after m repetitions. The precision of the estimators $\boldsymbol{\theta}_{\text{est}}$ is measured by $\boldsymbol{\Sigma}^{-1}$, the inverse of its $(d \times d)$–dimensional covariance matrix $\boldsymbol{\Sigma}$ with entries $\Sigma^{\mu\nu} = \text{Cov}(\theta^\mu_{\text{est}}, \theta^\nu_{\text{est}})$, $1 \leqslant \mu, \nu \leqslant d$. The CFI sets the upper bound of the precision, and the CFI itself is upper bounded by the QFI via the quantum Cramér-Rao inequality (QCRI) [14,15],

$$m\boldsymbol{\mathcal{F}} \geqslant m\boldsymbol{\mathcal{I}} \geqslant \boldsymbol{\Sigma}^{-1}; \tag{6}$$

this indicates $m\mathcal{F}_{\mu\mu} \geqslant m\mathcal{I}_{\mu\mu} \geqslant (\boldsymbol{\Sigma}^{-1})_{\mu\mu} = 1/\delta^2\theta^\mu_{\text{est}}$, when only one of the parameters, e.g., θ^μ as shown in Fig. 1, requires estimation. The saturation of the ultimate precision $m\mathcal{F}_{\mu\mu}$ requires optimization of the estimation and measurement: the last equality is reached by maximal likelihood estimation, and the first equality is reached by the optimal measurement $\hat{\boldsymbol{E}}$ satisfying [40]

$$|\psi\rangle\langle\psi|(\lambda_\mu - \hat{L}_\mu)\hat{E}_i^{1/2} = 0, \forall i, \tag{7}$$

with $\lambda_\mu \in \mathbb{R}$. $\hat{L}_\mu$ is the symmetric logarithmic derivative defined by $\hat{\partial}_\mu\hat{\rho} \equiv (\hat{L}_\mu\hat{\rho} + \hat{\rho}\hat{L}_\mu)/2$ with $\hat{\rho} = |\psi\rangle\langle\psi|$. We mention that the QCRI, Eq. (6), is still valid when $\hat{\rho}$ is a general mixed state [14,15,40].

C. Multiparameter estimation

In multiparameter cases, one needs to simultaneously estimate a set of parameters $\boldsymbol{\theta}$ from the given state $|\psi(\boldsymbol{\theta})\rangle$. The QCRI, Eq. (6), is still valid. However, to quantify the quality of measurement and estimation, one should extract a scalar index from the covariance matrix $\boldsymbol{\Sigma}$. The index in the traditional framework is $\text{tr}(\boldsymbol{G}\boldsymbol{\Sigma})$, the weighted average of the entries $\Sigma^{\mu\nu}$, by introduction of a $(d \times d)$–dimensional real symmetric positive cost matrix $\boldsymbol{G}$. It straightforwardly gives us the inequality

$$\text{tr}(\boldsymbol{G}\boldsymbol{\mathcal{F}}^{-1}) \leqslant \text{tr}(\boldsymbol{G}\boldsymbol{\mathcal{I}}^{-1}) \leqslant m\text{tr}(\boldsymbol{G}\boldsymbol{\Sigma}), \tag{8}$$

with the multiparameter quantum Cramér-Rao bound (QCRB) $\text{tr}(\boldsymbol{G}\boldsymbol{\mathcal{F}}^{-1})$. Without loss of generality, all of the components of $\boldsymbol{\theta}$ are assumed to be unknown and are independent of each other. This indicates that both $\boldsymbol{\mathcal{F}}$ and $\boldsymbol{\mathcal{I}}$ are full rank and completely positive. Specifically, when $\boldsymbol{G}$ is taken as the identity, the corresponding index is the trace of the covariance matrix, which has been widely used in recent studies

[3–6,9]. As a precision limit, the QCRB is too optimistic, as it is not necessarily attainable. For pure-state cases, the QCRB is saturable and only saturable by states $|\psi(\boldsymbol{\theta})\rangle$ with $\langle\psi(\boldsymbol{\theta})|[\hat{L}_\mu, \hat{L}_\nu]|\psi(\boldsymbol{\theta})\rangle = 0$, $\forall\mu, \nu$, i.e., the vanishing of the Berry curvature matrix. This is the *commutation condition* proved by Matsumoto [3]. The generalization of this condition to mixed states was first discussed for specific states [5,11,12,87], then proved for general cases via the Holevo Cramér-Rao bound with the local asymptotic normality theory [88] and direct minimization [6].

The asymptotically saturable bound of $\mathrm{tr}(\boldsymbol{G\Sigma})$ for the general state $\hat{\rho}(\boldsymbol{\theta})$ is the well-known Holevo Cramér-Rao bound [15] with the (equivalent) formulation [6,89]

$$\min_{\{X_\mu\}}\{\mathrm{tr}(\boldsymbol{G}\mathrm{Re}\boldsymbol{V}) + \mathrm{tr}(|\sqrt{\boldsymbol{G}}\mathrm{Im}\boldsymbol{V}\sqrt{\boldsymbol{G}}|)\} \leqslant m\mathrm{tr}(\boldsymbol{G\Sigma}), \tag{9}$$

where the $(d \times d)$–dimensional matrix $\boldsymbol{V}$ is defined with the entries $V_{\mu\nu} = \mathrm{Tr}(\hat{\rho}\hat{X}_\mu\hat{X}_\nu)$; the minimization is done over the set of Hermation matrices $\hat{X}_\mu$ satisfying $\mathrm{Tr}(\hat{\rho}\{\hat{X}_\mu, \hat{L}_\nu\}) = 2\delta_{\mu\nu}$. As mentioned by Ragy *et al.* [6], the saturation of this bound in general cases requires infinite copies of probe states and allowance of collective measurements. The minimum of $m\mathrm{tr}(\boldsymbol{G}\mathrm{Re}\boldsymbol{V})$ over the sets of $\{\hat{X}_\mu\}$ is exactly the QCRB [6,89]. Hence, the Holevo Cramér-Rao bound also plays significant roles in generalizations of the commutation condition to mixed states [6,87,88].

Much has been achieved [1,2,19–21] with these two bounds. Both of them are highly dependent on the cost matrix $\boldsymbol{G}$, which is introduced additionally to increase the flexibility of the index $\mathrm{tr}(\boldsymbol{G\Sigma})$ in solving specific problems accordingly. However, there is no straightforward method to grant them information-geometric interpretations as researchers have done in single-parameter cases.

III. DENSITY OF STATES

Riemannian geometry provides us a standard method to quantify the invariant volume and the corresponding density of a Riemannian manifold. If $\boldsymbol{g}$ serves as the metric of a Riemannian manifold $(M, \boldsymbol{g})$ with coordinates Θ, $dV = \sqrt{|\boldsymbol{g}|}d\Theta$ defines the invariant volume element of the manifold M, where $|\boldsymbol{g}|$ denotes the determinant of $\boldsymbol{g}$. The element dV is invariant under the change of coordinates. This indicates that $\sqrt{|\boldsymbol{g}|} = dV/d\Theta$ measures the intrinsic density of the manifold. Hence, in the framework of information geometry, one can formally define a measure of the density of states in a statistical manifold (projective Hilbert space) with $\sqrt{|\boldsymbol{g}^I|}$ $(\sqrt{|\boldsymbol{g}^F|})$. The two densities have ample physical implications. As we show below, they naturally emerge from the basic theory of multiparameter estimation as the bounds of the precision measure.

A. Volume of estimators and density of distinguishable states

In multiparameter estimation, researchers simultaneously estimate a set of d independent parameters, i.e., the *estimand* $\boldsymbol{\theta}$ from the distribution $\boldsymbol{p}(\boldsymbol{\theta}) = (p_0, p_1, \ldots, p_n)$, with $p_i = \langle\psi(\boldsymbol{\theta})|\hat{E}_i|\psi(\boldsymbol{\theta})\rangle$. After m repetitions of trails, one acquires a sample with m measurement results, in which the outcome i occurs at frequency ξ_i. According to the central limit theorem, the distribution of the frequency $\boldsymbol{\xi} = (\xi_0, \xi_1, \ldots, \xi_n)$ converges to a Gaussian distribution,

$$\rho(\boldsymbol{\xi}|\boldsymbol{\theta}) \propto \exp\left[-\frac{m}{2}\sum_i \frac{(p_i - \xi_i)^2}{p_i}\right], \tag{10}$$

with $m \to \infty$. This distribution is highly localized in the neighborhood of the true value $\boldsymbol{p}(\boldsymbol{\theta})$. It is natural to conjecture that there exists a set of unbiased estimators $\bar{\boldsymbol{\theta}}_{\mathrm{est}}(\boldsymbol{\xi})$ such that with the repetition $m \to \infty$, the distribution $\rho(\bar{\boldsymbol{\theta}}_{\mathrm{est}}|\boldsymbol{\theta})$ is asymptotic to

$$\rho(\bar{\boldsymbol{\theta}}_{\mathrm{est}}|\boldsymbol{\theta}) \propto \exp\left[-\frac{4m}{2}(\bar{\boldsymbol{\theta}}_{\mathrm{est}} - \boldsymbol{\theta})^T\boldsymbol{g}^I(\bar{\boldsymbol{\theta}}_{\mathrm{est}} - \boldsymbol{\theta})\right] \tag{11}$$

in the neighborhood of $\boldsymbol{\theta}$, where the linear approximation $p_i - \xi_i \approx \partial_\mu p_i(\theta^\mu - \bar{\theta}^\mu_{\mathrm{est}})$ is valid. The validity of this conjecture in the whole parameter space relates to the topics of asymptotic normality of estimation, where $\bar{\boldsymbol{\theta}}_{\mathrm{est}}$ with the distribution from Eq. (11) are called asymptotically efficient estimators. Roots of likelihood equations and maximum likelihood estimation are proved efficient asymptotically under regularity conditions [90,91] (for details, see Appendix A) which can be locally satisfied by most statistical models in quantum metrology.

Two Gaussian distributions can be reliably discriminated when their overlap is less than a specific value, as shown in Fig. 1(c) and [39]. The distribution $\rho(\bar{\boldsymbol{\theta}}_{\mathrm{est}}|\boldsymbol{\theta})$ thus acquires an effective width along a given curve $\boldsymbol{\theta}(t)$. This indicates that a finite number of states are distinguishable on a segment of the curve. This is the core ingredient of the statistical distance [39]. For general unbiased estimators $\boldsymbol{\theta}_{\mathrm{est}}$, the FRM $\boldsymbol{g}^I$ still bounds the inverse of their covariance matrix $\boldsymbol{\Sigma}$ as shown by the QCRI, Eq. (6). This indicates that the distribution of $\boldsymbol{\theta}_{\mathrm{est}}$ is still highly localized. The variance $\boldsymbol{\Sigma}$ is still a qualified measure of $\boldsymbol{\theta}_{\mathrm{est}}$'s uncertainty, with the repetition $m \to \infty$. Consistent with the statistical distance [39], we take the width of $\rho(\boldsymbol{\theta}_{\mathrm{est}}|\boldsymbol{\theta})$ along the curve $\boldsymbol{\theta}(t)$ as $2\delta t$, with the variance $\delta t \equiv [\dot{\boldsymbol{\theta}}^T\boldsymbol{\Sigma}\dot{\boldsymbol{\theta}}]^{1/2}$, as illustrated in Fig. 1(c).

In multiparameter cases as shown in Fig. 2(c), all of the d components of $\boldsymbol{\theta}$ are assumed to be unknown. The distribution $\rho(\boldsymbol{\theta}_{\mathrm{est}}|\boldsymbol{\theta})$ expands in all directions, hence endowing an effective volume in the d-dimensional parameter space. Because the covariance matrix is a primary measure of the estimators' uncertainty, we take $V_E(\boldsymbol{\theta}_{\mathbf{est}}) \equiv \sqrt{|4\boldsymbol{\Sigma}|}$ as a measure of the volume of the distribution $\rho(\boldsymbol{\theta}_{\mathrm{est}}|\boldsymbol{\theta})$, henceforth $\boldsymbol{p}(\boldsymbol{\theta})$. The number of states distinguishable in the neighborhood $d\Theta$ of point $\boldsymbol{\theta}$ is thus measured by $d\Theta/V_E(\boldsymbol{\theta}_{\mathrm{est}})$. This is vivid in the diagonal coordinates $\boldsymbol{\zeta}$ of the covariance matrix $\boldsymbol{\Sigma}$, where the estimators' volume equals $\Pi_\mu 2\delta\zeta^\mu$. $\Pi_\mu n^\mu$ states can be distinguished reliably in a volume element $\Pi_\mu d\zeta^\mu$ totally, with $n^\mu = d\zeta^\mu/2\delta\zeta^\mu$ states distinguishable from the increment $d\zeta^\mu$.

Based on the above discussion, we define $\sqrt{|\boldsymbol{g}^I|}$ as the local *density of distinguishable states* (DDS) $\mathcal{D}_D(\boldsymbol{\theta})$ in the neighborhood of point $\boldsymbol{\theta}$. The DDS measures the maximal density of estimators $\boldsymbol{\theta}$, i.e., quantum states $|\psi(\boldsymbol{\theta})\rangle$, distinguishable in a single-shot measurement with

$$m^{d/2}\mathcal{D}_D(\boldsymbol{\theta}) \equiv m^{d/2}\sqrt{|\boldsymbol{g}^I|} \geqslant \frac{1}{V_E(\boldsymbol{\theta}_{\mathrm{est}})}, \tag{12}$$

where the constant $m^{d/2}$ denotes the enhancement of repetitions, and equality is reached by efficient estimators $\bar{\boldsymbol{\theta}}$ with

$1/(4\mathbf{\Sigma}) = m\boldsymbol{g}^I$. The proof is given with the QCRI in Eq. (15). Furthermore, we mention that $\sqrt{|\mathcal{I}|}d\Theta$ is also well known as the Jeffreys prior [92–95] in Bayesian estimation. It is the noninformative prior distribution in the parameter space Θ.

B. Intrinsic density of quantum states

Like the FRM, the QFM $\boldsymbol{g}^F$ serves as the metric of the projective Hilbert spaces $\mathbb{C}\mathbf{P}^n$, and $\sqrt{|\boldsymbol{g}^F|}$ measures the *intrinsic density of quantum states* (IDQS) in $\mathbb{C}\mathbf{P}^n$ with

$$\mathcal{D}_Q(\boldsymbol{\theta}) \equiv \sqrt{|\boldsymbol{g}^F|} = dV_Q/d\Theta, \tag{13}$$

where dV_Q denotes the invariant volume element of $\mathbb{C}\mathbf{P}^n$. The form of the IDQS is invariant under reparametrization, and its value is invariant under SU(N) rotation in Hilbert spaces. The IDQS depicts the "uniformity" of $\mathbb{C}\mathbf{P}^n$. For each point $\boldsymbol{\theta}$ in the parameter space Θ, there exists a projector $|\psi(\boldsymbol{\theta})\rangle\langle\psi(\boldsymbol{\theta})|$ that illustrates the projection to states $|\psi(\boldsymbol{\theta})\rangle$ in projective Hilbert spaces. Together with the IDQS serving as the intrinsic measure, one can define a projector to the projective Hilbert spaces with

$$\hat{\mathbb{1}} \propto \int d\Theta \mathcal{D}_Q(\boldsymbol{\theta})|\psi(\boldsymbol{\theta})\rangle\langle\psi(\boldsymbol{\theta})| \tag{14}$$

if the map $\boldsymbol{\theta} \to |\psi(\boldsymbol{\theta})\rangle\langle\psi(\boldsymbol{\theta})|$ is an isomorphism between Θ and $\mathbb{C}\mathbf{P}^n$. It is indeed the completeness relation, or decomposition of $\hat{\mathbb{1}}$ of the projective Hilbert spaces [36]. A sketch of the proof of Eq. (14) is given in Appendix B.

In practical studies, one often deals with a class of states, such as coherent states and spin-squeezed states, which composes a submanifold of the projective Hilbert spaces. The density of quantum states is inherited from $\mathbb{C}\mathbf{P}^n$ together with the induced metric. Hence if a class of parameterized states is complete (overcomplete), one may calculate the completeness relation with Eq. (14) by integrating over the parameter space Θ. Examples of coherent states and squeezed states as submanifolds of $\mathbb{C}\mathbf{P}^\infty$ are given in Appendix C. It is a new method that can significantly decrease the complexity of calculating the completeness.

IV. QCRI IN DETERMINANT FORM, ATTAINABILITY OF THE IDQS, AND THE GAP BETWEEN THE IDQS AND THE MAXIMAL DDS

A. QCRI in determinant form and attainability of the IDQS

Via quantification of the density of states attained in a given measurement, the DDS serves as a measure of the measurement's quality in multiparameter estimation. And the IDQS upper bounds the DDS over the sets of POVMs for a given quantum state. Specifically, we can generalize the QCRI, Eq. (6), to the determinant form, which indicates

$$\mathcal{D}_Q(\boldsymbol{\theta}) \geqslant \mathcal{D}_D(\boldsymbol{\theta}) \geqslant \frac{1}{m^{d/2}V_E(\boldsymbol{\theta}_{\mathbf{est}})}, \tag{15}$$

where the first (second) equality is reached if and only if the metric $\boldsymbol{g}^I = \boldsymbol{g}^F$ ($\boldsymbol{g}^I = (4m\mathbf{\Sigma})^{-1}$).

Proof. We begin with two arbitrary positive definite real symmetric matrices, $\boldsymbol{A}$ and $\boldsymbol{B}$, which satisfy the matrix inequality $\boldsymbol{A} \geqslant \boldsymbol{B}$, i.e.,

$$\boldsymbol{A} - \boldsymbol{B} \geqslant \mathbf{0}. \tag{16}$$

One can diagonalize the difference matrix with a unitary matrix $\boldsymbol{U}$. Denoting $\boldsymbol{U}\boldsymbol{M}\boldsymbol{U}^{-1} = \boldsymbol{M}'$, $\boldsymbol{M} = \boldsymbol{A}, \boldsymbol{B}$, we have

$$\boldsymbol{C} \equiv \boldsymbol{A}' - \boldsymbol{B}' = \mathrm{diag}[\lambda_1, \lambda_2, \ldots, \lambda_d], \tag{17}$$

with the eigenvalue $\lambda_i \geqslant 0$, for all i. As $\boldsymbol{B}'$ is positive definite, we have $|[\boldsymbol{B}']^{ij\cdots}| > 0$, where $[\boldsymbol{B}']^{ij\cdots}$ is the algebraic complement of $\{B'_{ii}, B'_{jj}, \ldots\}$. Therefore, we have the determinant

$$\begin{aligned} |\boldsymbol{A}'| &= |\boldsymbol{B}' + \boldsymbol{C}| \\ &= |\boldsymbol{B}'| + \lambda_i|[\boldsymbol{B}']^i| + \lambda_i\lambda_j|[\boldsymbol{B}']^{ij}| + \ldots + \Pi_i\lambda_i \\ &\geqslant |\boldsymbol{B}'|, \end{aligned} \tag{18}$$

which indicates

$$|\boldsymbol{A}| \geqslant |\boldsymbol{B}| = 1/|\boldsymbol{B}^{-1}|. \tag{19}$$

The equality holds iff $\lambda_i = 0, \forall i$, i.e., $\boldsymbol{A} = \boldsymbol{B}$. By setting $\boldsymbol{A} = \boldsymbol{g}^F$ and $\boldsymbol{B} = \boldsymbol{g}^I$ [$\boldsymbol{A} = \boldsymbol{g}^I$ and $\boldsymbol{B} = (4m\mathbf{\Sigma})^{-1}$], the first (second) inequality in Eq. (15) is thus proved. ■

Importantly, the saturation of $\mathcal{D}_Q(\boldsymbol{\theta})$ indicates that the metric $\boldsymbol{g}^I$ equals $\boldsymbol{g}^F$ exactly. Under this property, the densities of quantum states are distinguished from other precision measures. Specifically, one can extract an alternative precision measure, $f(\boldsymbol{g}^I)$, from the metric $\boldsymbol{g}^I$ via a proper function, f, then define the corresponding bounds $f(\boldsymbol{g}^F)$ according to the QCRI. However, the fundamentality of the IDDS and DDS makes $\mathcal{D}_D(\boldsymbol{\theta}) = \mathcal{D}_Q(\boldsymbol{\theta})$ a sufficient condition for the saturation of all of these bounds, which reads $f(\boldsymbol{g}^I) = f(\boldsymbol{g}^F)$. From this point of view, the $D_Q(\boldsymbol{\theta})$ measures all of the local information stored in the metric $\boldsymbol{g}^F$, and the density $\mathcal{D}_D(\boldsymbol{\theta})$ is capable of detecting any difference between the two metrics.

Physically, Eq. (15) depicts the ability to infer the density of quantum states via a quantum measurement. In single-parameter cases, the upper bound defined by the QFM is exact, as shown by Eq. (6). This indicates that one can infer the QFM entries $\mathcal{F}_{\mu\mu}$ via the quantum measurement without the loss of distinguishability of the quantum states. However, the situation for the IDQS in multiparameter cases is more complicated, as shown below.

B. Gap between the maximal DDS and the IDQS

To attain the IDQS in Eq. (15) for a given state, one should perform a measurement that is simultaneously optimal for all of the components of parameters $\boldsymbol{\eta}$, the diagonal coordinates of QFM $\boldsymbol{g}^F$. However, such a measurement does not always exist for a general state $|\psi(\boldsymbol{\eta})\rangle$. The critical point is that the optimal measurements of each specific component η^μ may noncommute with each other. The attainability condition is consistent with the well-known compatibility condition [3,6,8], which states that the optimal measurements corresponding to two parameters θ^μ and θ^ν are compatible only if the Berry curvatures $\mathcal{B}_{\mu\nu} \equiv \langle\psi(\boldsymbol{\eta})|[\hat{L}_\mu, \hat{L}_\nu]|\psi(\boldsymbol{\eta})\rangle/4$ vanish in state $|\psi(\boldsymbol{\eta})\rangle$. It also indicates that the IDQS is only attainable for states $|\psi(\boldsymbol{\eta})\rangle$ with vanishing Berry curvatures $\mathcal{B}_{\mu\nu}, \forall\mu, \nu$.

For states with a nonzero Berry curvature, the maximal DDS attained over the measurements is smaller than the corresponding IDQS. A gap between the maximal DDS and the

IDQS is induced by the incompatibility of the optimal measurements of those parameters. The gap generally depends on both the QFI and the Berry curvature. However, specific to the three-level system with two parameters, we show that some of the characteristics of the gap are solely quantified by elements of the Berry curvature.

V. THREE-LEVEL SYSTEMS

To study the gap between the maximal DDS and the IDQS, we need at least two independent parameters identifiable via parameter estimation. Specific for projective measurements, it indicates that the minimal quantum system is three-level. They can support ternary-outcome measurements and induce the classical distribution located in a two-simplex, as shown in Fig. 2. The projective Hilbert space $\mathbb{C}\mathbf{P}^2$ of the three-level system is four-dimensional in real coordinates, i.e., the pure state of these systems has four independent parameters. We study its two-dimensional submanifolds by fixing the other two parameters of the four.

A. Vertex measurements

Even in single-parameter cases, finding a measurement scheme optimal for arbitrary given states is complicated. However, if sufficient prior information is provided, one can apply an asymptotically optimal measurement scheme: projective measurement $\hat{\boldsymbol{E}}^v(\theta^\mu)$ with the state $|\psi(\theta^\mu)\rangle\langle\psi(\theta^\mu)| \in \hat{\boldsymbol{E}}^v(\theta^\mu)$ is asymptotically optimal for the given state $|\psi(\theta^\mu + \delta\theta^\mu)\rangle$ with the mismatch $\delta\theta^\mu$ approaching 0. In multiparameter estimation, Humphreys *et al.* [4] and Pezzé *et al.* [8] prove that $\hat{\boldsymbol{E}}^v(\boldsymbol{\theta}) \equiv \{|\Upsilon_i\rangle\langle\Upsilon_i|\}$, with $|\Upsilon_0\rangle \sim |\psi(\boldsymbol{\theta})\rangle$, $\langle\Upsilon_i|\Upsilon_j\rangle = \delta_{ij}$, and $\sum_i |\Upsilon_i\rangle\langle\Upsilon_i| = \hat{\mathbb{1}}$, is also asymptotically optimal for state $|\psi(\boldsymbol{\theta}+\delta\boldsymbol{\theta})\rangle$ with zero Berry curvature [2]. For the distribution of its measurement results $\boldsymbol{p}$ is located in the neighborhood of the vertex $(1, 0, 0, \dots)$ of the simplex, we denote $\hat{\boldsymbol{E}}^v(\boldsymbol{\theta})$ the *vertex measurement* for state $|\psi(\boldsymbol{\theta}+\delta\boldsymbol{\theta})\rangle$ in this article for convenience. For the parameter θ^μ, there exists an informative vertex measurement,

$$\hat{\boldsymbol{E}}^\mu(\boldsymbol{\theta}) = \{|\psi(\boldsymbol{\theta})\rangle\langle\psi(\boldsymbol{\theta})|, |\nabla_\mu\psi\rangle\langle\nabla_\mu\psi|, |\Upsilon_2\rangle\langle\Upsilon_2|, \dots\}, \tag{20}$$

where $|\nabla_\mu\psi\rangle \equiv \hat{\nabla}_\mu|\psi(\boldsymbol{\theta})\rangle/\lambda_\mu$ denotes the "direction of speed" of state $|\psi(\boldsymbol{\theta})\rangle$'s movement in projective Hilbert spaces induced by the shift of the parameter θ^μ; the norm $\lambda_\mu = (g^F_{\mu\mu})^{1/2}$ is the corresponding "velocity." Furthermore, $|\Upsilon_2\rangle\langle\Upsilon_2|, \dots$ make no contribution to the estimation of $\delta\theta^\mu$ in single-parameter estimation, for the movements are confined in the subspaces spanned by $|\psi(\theta^\mu)\rangle$ and $|\nabla_\mu\psi(\theta^\mu)\rangle$.

1. General cases

For state $|\psi(\boldsymbol{\theta})\rangle$ of the three-level system with two parameters, $\boldsymbol{\theta} = (\theta^1, \theta^2)$, the two "optimal directions" $|\nabla_1\psi\rangle$ and $|\nabla_2\psi\rangle$ are nonorthogonal generally. They interfere with each other in the projective measurement. The attainable DDS is thus decreased. Specifically, for a given state $|\psi(\boldsymbol{\theta}_0)\rangle$, we have the following property: *The maximal DDS attained by the vertex measurements (MvDDS) equals the square root of the quantum geometric tensor's determinant, i.e.,*

$$\max_{\{\hat{\boldsymbol{E}}^v\}}[\mathcal{D}_D]^2 = |\mathcal{Q}| = \mathcal{D}_Q^2 - \mathcal{B}_{12}^2/4, \tag{21}$$

where the maximization is done over the sets of vertex measurements $\{\hat{\boldsymbol{E}}^v(\boldsymbol{\theta})\}$ where $\boldsymbol{\theta}$ approaches $\boldsymbol{\theta}_0$. It also indicates that the square gap between the IDQS and the MvDDS, i.e., the unattainable square density of quantum states, is proportional to the square of the Berry curvature. Next, we prove Eq. (21) in general cases, then exemplify it with the SU(3) parametrization in Sec. VA2.

Proof. We prove this property with its equivalent proposition: the maximal DDS acquired over the set of vertex measurements $\{\hat{\boldsymbol{E}}^v(\boldsymbol{\theta})\}$ in the neighborhood of state $|\psi(\boldsymbol{\theta}+\delta\boldsymbol{\theta})\rangle$ converges to $\sqrt{|\mathcal{Q}(\boldsymbol{\theta})|}$ with the mismatches $\delta\boldsymbol{\theta}$ approaching 0. Specifically, we fix the parameters $\boldsymbol{\theta}$ of the vertex measurement $\hat{\boldsymbol{E}}^v(\boldsymbol{\theta})$, then substitute $\boldsymbol{\theta}_0$ with $\boldsymbol{\theta}+\delta\boldsymbol{\theta}$ to study the DDS acquired in the neighborhood of state $|\psi(\boldsymbol{\theta}+\delta\boldsymbol{\theta})\rangle$. The maximization should be done over both sets of vertex measurements $\{\hat{\boldsymbol{E}}^v(\boldsymbol{\theta})\}$, i.e., $\{|\Upsilon_1\rangle, |\Upsilon_2\rangle\}$, and the mismatches $\delta\boldsymbol{\theta}$.

We begin with the assumption that the mismatches $\delta\boldsymbol{\theta}$ are small enough to validate the linear approximation

$$|\psi(\boldsymbol{\theta}+\delta\boldsymbol{\theta})\rangle \approx |\psi(\boldsymbol{\theta}+\delta\boldsymbol{\theta})\rangle_1 \equiv c_0|\psi(\boldsymbol{\theta})\rangle + \delta\theta^\mu\hat{\nabla}_\mu|\psi(\boldsymbol{\theta})\rangle, \tag{22}$$

with $c_0 \in \mathbb{C}$, $\mu = 1, 2$. The overlap of the two derivatives is denoted $\langle\nabla_1\psi|\nabla_2\psi\rangle = \cos\alpha e^{i\beta}, 0 \leqslant \alpha \leqslant \pi/2, 0 \leqslant \beta < 2\pi$. The corresponding quantum geometric tensor is

$$\mathcal{Q}(\boldsymbol{\theta}) = \begin{bmatrix} \lambda_1\lambda_1 & \lambda_1\lambda_2\cos\alpha e^{i\beta} \\ \lambda_1\lambda_2\cos\alpha e^{-i\beta} & \lambda_2\lambda_2 \end{bmatrix}, \tag{23}$$

with the determinant $|\mathcal{Q}(\boldsymbol{\theta})| = \lambda_1^2\lambda_2^2\sin^2\alpha$.

First, we prove

$$\mathcal{D}_D(\boldsymbol{\theta}+\delta\boldsymbol{\theta})\big|^2_{\delta\boldsymbol{\theta}\to\boldsymbol{0}} \leqslant |\mathcal{Q}(\boldsymbol{\theta})| \tag{24}$$

by introducing the polar parameters $\boldsymbol{\eta} = (r, \theta_\chi)$ with

$$\delta\theta^1\lambda_1 = r\cos\theta_\chi, \qquad \delta\theta^2\lambda_2 = r\sin\theta_\chi, \tag{25}$$

$r \geqslant 0$, and $0 \leqslant \theta_\chi < 2\pi$. In the basis of the vertex measurement $\hat{\boldsymbol{E}}^v(\boldsymbol{\theta})$, we have the expansion

$$|\psi(\boldsymbol{\theta}+\delta\boldsymbol{\theta})\rangle_1 = c_0|\psi(\boldsymbol{\theta})\rangle + \sum_{i=1,2} x_i e^{i\phi_i}|\Upsilon_i\rangle, \tag{26}$$

with $x_i e^{i\phi_i} = r[\cos\theta_\chi\langle\Upsilon_i|\nabla_1\psi\rangle + \sin\theta_\chi\langle\Upsilon_i|\nabla_2\psi\rangle], x_i \geqslant 0$, and $0 \leqslant \phi_i < 2$, as functions of $\boldsymbol{\eta}$. For the parameter η^μ, we define an alternative derivative,

$$\begin{aligned}\tilde{\nabla}_\mu|\psi(\boldsymbol{\theta})\rangle &\equiv (\hat{\mathbb{1}} - |\psi(\boldsymbol{\theta})\rangle\langle\psi(\boldsymbol{\theta})|)\tilde{\partial}_\mu|\psi(\boldsymbol{\theta}+\delta\boldsymbol{\theta})\rangle_1 \\ &= \sum_{i=1,2}(\tilde{\partial}_\mu x_i + i\tilde{\partial}_\mu\phi_i x_i)e^{i\phi_i}|\Upsilon_i\rangle, \end{aligned} \tag{27}$$

with $\tilde{\partial}_\mu \equiv \partial/\partial\eta^\mu$. Obviously, the two kinds of derivatives are connected with a Jacobian $\boldsymbol{J} \equiv (\partial\boldsymbol{\eta}/\partial\boldsymbol{\theta})$ as

$$\begin{bmatrix}\nabla_1 \\ \nabla_2\end{bmatrix} = \boldsymbol{J}^T\begin{bmatrix}\tilde{\nabla}_1 \\ \tilde{\nabla}_2\end{bmatrix}. \tag{28}$$

Because the parameter $\eta^1 = r$ only relates to the modulus $\{x_i\}$, we have $\tilde{\partial}_1\phi_i = 0$, with $i = 1, 2$. Hence, the corresponding "quantum geometric tensor" can be simplified as

$$\tilde{\mathcal{Q}} = \begin{bmatrix} \tilde{g}_{11} & \tilde{g}_{12} + i\sum_i \tilde{\partial}_1 x_i \tilde{\partial}_2\phi_i x_i \\ \tilde{g}_{12} - i\sum_i \tilde{\partial}_1 x_i \tilde{\partial}_2\phi_i x_i & \tilde{g}_{22} + \sum_i \tilde{\partial}_2\phi_i \tilde{\partial}_2\phi_i x_i^2 \end{bmatrix}, \quad (29)$$

with $\tilde{\mathcal{Q}}_{\mu\nu} \equiv \langle\psi(\boldsymbol{\theta})|\overleftarrow{\tilde{\nabla}}_\mu \tilde{\nabla}_\nu|\psi(\boldsymbol{\theta})\rangle$ and

$$\tilde{g}_{\mu\nu} \equiv \sum_{i=1,2} \tilde{\partial}_\mu x_i \tilde{\partial}_\nu x_i. \quad (30)$$

Based on Eq. (29), we have the difference

$$|\tilde{\mathcal{Q}}| - |\tilde{\boldsymbol{g}}| = \tilde{g}_{11}\sum_{i=1,2}\tilde{\partial}_2\phi_i\tilde{\partial}_2\phi_i x_i^2 - \left(\sum_{i=1,2}\tilde{\partial}_1 x_i \tilde{\partial}_2\phi_i x_i\right)^2 \geqslant 0, \quad (31)$$

where the equality is reached by $|\psi(\boldsymbol{\theta}+\delta\boldsymbol{\theta})\rangle_1$ with $\tilde{\partial}_1 x_1/\tilde{\partial}_1 x_2 = \tilde{\partial}_2\phi_1 x_1/(\tilde{\partial}_2\phi_2 x_2)$, i.e.,

$$\tilde{\partial}_2(\phi_1 - \phi_2) = 0, \quad (32)$$

attained via $\tilde{\partial}_1 x_i = x_i/r$. Together with $\tilde{\partial}_1(\phi_1 - \phi_2) = 0$, this condition indicates that the relative phase $(\phi_1 - \phi_2)$ is constant in the neighborhood of state $|\psi(\boldsymbol{\theta}+\delta\boldsymbol{\theta})\rangle$.

With the mismatches $\delta\boldsymbol{\theta} \to 0$, $\tilde{g}_{\mu\nu}$ converges to the entry of the FRM $\tilde{g}^I{}_{\mu\nu}(\boldsymbol{\theta}+\delta\boldsymbol{\theta})$, where the term $\tilde{\partial}_\mu p_0 \tilde{\partial}_\nu p_0/p_0$ with $p_0 = |c_0|^2$ is null, as $\partial_\mu p_0$ is first-order infinitesimal and $p_0 \to 1$. Then premultiplying $\boldsymbol{J}^T$ and postmultiplying $\boldsymbol{J}$ on both sides of Eq. (31), we have $\boldsymbol{J}^T\tilde{\mathcal{Q}}\boldsymbol{J} = \mathcal{Q}(\boldsymbol{\theta})$ and $\boldsymbol{J}^T\tilde{\boldsymbol{g}}^I(\boldsymbol{\theta}+\delta\boldsymbol{\theta})\boldsymbol{J} = \boldsymbol{g}^I(\boldsymbol{\theta}+\delta\boldsymbol{\theta})$. The inequality, Eq. (24), is thus proved.

Next, we show the attainability of Eq. (24) via a specific measurement,

$$\hat{\boldsymbol{E}}^1(\boldsymbol{\theta}) = \{|\psi(\boldsymbol{\theta})\rangle\langle\psi(\boldsymbol{\theta})|, |\nabla_1\psi\rangle\langle\nabla_1\psi|, |\Upsilon_2\rangle\langle\Upsilon_2|\}, \quad (33)$$

with $|\Upsilon_2\rangle = (|\nabla_2\psi\rangle - \cos\alpha e^{i\beta}|\nabla_1\psi\rangle)/\sin\alpha$. In this basis, we have the coefficients

$$\begin{aligned} x_1 e^{i\phi_1} &= r[\cos\theta_\chi + \sin\theta_\chi\cos\alpha e^{i\beta}], \\ x_2 e^{i\phi_2} &= r\sin\theta_\chi\sin\alpha. \end{aligned} \quad (34)$$

Condition (32) is satisfied by states $|\psi(\boldsymbol{\theta}+\delta\boldsymbol{\theta})\rangle$ with $\theta_\chi = 0$, i.e., $|\delta\theta^2\lambda_2|/|\delta\theta^1\lambda_2| = 0$. The corresponding FRM with respect to the parameters (θ^1, θ^2) is

$$\boldsymbol{g}^I(\boldsymbol{\theta}+\delta\boldsymbol{\theta})|_{\delta\boldsymbol{\theta}\to\boldsymbol{0}} = \begin{bmatrix} \lambda_1^2 & \lambda_1\lambda_2\cos\alpha\cos\beta \\ \lambda_1\lambda_2\cos\alpha\cos\beta & \lambda_2^2(\sin^2\alpha + \cos^2\alpha\cos^2\beta) \end{bmatrix}, \quad (35)$$

and the determinant $|\boldsymbol{g}^I(\boldsymbol{\theta}+\delta\boldsymbol{\theta})| \to |\mathcal{Q}(\boldsymbol{\theta})| = \lambda_1^2\lambda_2^2\sin^2\alpha$, with $\delta\boldsymbol{\theta} \to \boldsymbol{0}$. This indicates that the measurement $\hat{\boldsymbol{E}}^1(\boldsymbol{\theta})$ asymptotically attains the MvDDS for states in the neighborhood of $|\psi(\boldsymbol{\theta}+\delta\boldsymbol{\theta})\rangle$ with $|\delta\theta^2\lambda_2|/|\delta\theta^1\lambda_1| \approx 0$ and $|\delta\theta^1\lambda_1| \to 0$. Together with the inequality, Eq. (24), we have thus proved Eq. (21). ∎

2. SU(3) parametrization

We parametrize the three-level system with

$$|\psi(\boldsymbol{\theta})\rangle = e^{i(\alpha+\gamma)}\cos\beta\sin\theta|1\rangle - e^{-i(\alpha-\gamma)}\sin\beta\sin\theta|2\rangle + \cos\theta|3\rangle, \quad (36)$$

where the parameters $\boldsymbol{\theta} = (\alpha, \gamma, \beta, \theta)$ are the Euler coordinates of the SU(3) group [96,97] with the global phase removed, and the range is modified to $-\pi \leqslant \alpha+\gamma < \pi$, $-\pi \leqslant \alpha-\gamma < \pi$ and $0 \leqslant \beta, \theta \leqslant \pi/2$ to cover the whole $\mathbb{C}\mathbf{P}^2$. Via a detailed calculation, we have the quantum geometric tensor of $|\psi(\boldsymbol{\theta})\rangle$:

$$\mathcal{Q}^{(\boldsymbol{\theta})} = \begin{bmatrix} \sin^2\theta(1-\cos^2 2\beta\sin^2\theta) & \cos 2\beta\sin^2\theta\cos^2\theta & i\sin 2\beta\sin^2\theta & -i\cos 2\beta\sin\theta\cos\theta \\ \cos 2\beta\sin^2\theta\cos^2\theta & \sin^2\theta\cos^2\theta & 0 & -i\sin\theta\cos\theta \\ -i\sin 2\beta\sin\theta^2 & 0 & \sin^2\theta & 0 \\ i\cos 2\beta\sin\theta\cos\theta & i\sin\theta\cos\theta & 0 & 1 \end{bmatrix}. \quad (37)$$

First, we have the complete relationship

$$\int_\Theta d^4\boldsymbol{\theta}\mathcal{D}_Q(\boldsymbol{\theta})|\psi(\boldsymbol{\theta})\rangle\langle\psi(\boldsymbol{\theta})| = \frac{\pi^2}{6}\hat{\mathbb{1}} \quad (38)$$

as an example of Eq. (14), with the IDQS $\mathcal{D}_Q(\boldsymbol{\theta}) = \sin 2\beta\sin^3\theta\cos\theta$. Under this parametrization, we have three two-dimensional submanifolds, $\Theta^{(\alpha\beta)}$, $\Theta^{(\alpha\theta)}$, and $\Theta^{(\gamma\theta)}$, with nonzero Berry curvature. We focus on the gap between the IDQS and the MvDDS with these submanifolds.

We calculate the MvDDS of states in each of these submanifolds numerically by optimizing the DDS of the sample states over the set of ternary-outcome vertex measurements $\hat{\boldsymbol{E}}^v$. With the numerical results, we illustrate the codistribution of the IDQS, Berry curvature, and MvDDS in Fig. 3. Each of the data points denotes a sample quantum state. All of the data points are located on the plane given by Eq. (21). This indicates that the square of MvDDS equals the determinant of the quantum geometric tensor, i.e., the unattainable square density of quantum states proportional to the square of the Berry curvature.

B. General projective measurements

The gap between the IDQS and the maximal DDS attained over the general projective measurement (MDDS) is too complicated for analytical study. Hence, we first study it numerically instead. We still focus on the three-level system with the SU(3) parametrization, Eq. (36). Corresponding to Fig. 3, we numerically optimize the DDS for states in submanifolds $\Theta^{(\alpha\beta)}$, $\Theta^{(\alpha\theta)}$, and $\Theta^{(\gamma\theta)}$ over the ternary-outcome projective measurements $\hat{\boldsymbol{E}} = \{|k_i\rangle\langle k_i||i = 0, 1, 2\}$. The numerical result is shown as the codistribution of the IDQS, Berry curvature, and MDDS in Fig. 4. It shows that all of the data points are located on or above the plane, which indicates

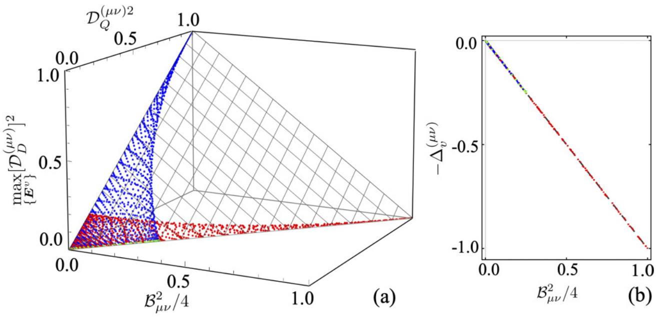

FIG. 3. Codistribution of the IDQS ($\mathcal{D}_Q^{(\mu\nu)}$), MvDDS ($\max_{\{\hat{E}^v\}}[\mathcal{D}_D^{(\mu\nu)}]$), and Berry curvature ($\mathcal{B}_{\mu\nu}$). The MvDDS is acquired via numerical optimization. (a) Red, blue, and green dots denote states in the submanifolds $\Theta^{(\alpha\beta)}$, $\Theta^{(\alpha\theta)}$, and $\Theta^{(\gamma\theta)}$, respectively. The plane is given by Eq. (21). (b) Gap between the IDQS and the MvDDS ($\Delta_v^{(\mu\nu)}$) vs the Berry curvature ($\mathcal{B}_{\mu\nu}$). The square gap is defined by $\Delta_v^{(\mu\nu)} = \mathcal{D}_Q^{(\mu\nu)2} - \max_{\{\hat{E}^v\}}[\mathcal{D}_D^{(\mu\nu)}]^2$.

that

$$\max_{\{\hat{E}\}}\left[\mathcal{D}_D^{(\mu\nu)}\right]^2 \geqslant \mathcal{D}_Q^{(\mu\nu)2} - \frac{3}{16}\mathcal{B}_{\mu\nu}^2 \tag{39}$$

numerically. Here, we treat the analytical validity of Eq. (39) as an *ansatz*. Data points on this numerical lower bound are given by states with $\mathcal{D}_Q^{(\mu\nu)} = |\mathcal{B}_{\mu\nu}|/2$, i.e., vanishing $|\mathcal{Q}|$. This means that the Berry curvature still characterizes the square gap between the IDQS and the MDDS.

Actually, we can prove that *the lower bound of the MDDS given in Eq. (39) is saturated by general two-parameter states with vanishing* $|\mathcal{Q}|$.

Proof. In the form of Eq. (23), the vanishing of $|\mathcal{Q}|$ indicates that $\alpha = 0$, i.e.,

$$|\nabla_2\psi\rangle = e^{i\beta}|\nabla_1\psi\rangle, \tag{40}$$

and $|\boldsymbol{g}^F| = \mathcal{B}_{12}^2/4 = \lambda_1^2\lambda_2^2\sin^2\beta$. We denote the overlap

$$\frac{\langle k_i|\nabla_1\psi\rangle\langle\psi|k_i\rangle}{|\langle\psi|k_i\rangle|} \equiv r_i e^{i(\theta_i-\beta/2)}, \tag{41}$$

with $r_i \geqslant 0$, $\sum_i r_i^2 = 1$, and $\theta_i \in [0, 2\pi)$. Together with Eq. (5) and the derivatives

$$\partial_\mu p_i = \langle k_i|\partial_\mu(|\psi\rangle\langle\psi|)|k_i\rangle = \langle k_i|\nabla_\mu(|\psi\rangle\langle\psi|)|k_i\rangle, \tag{42}$$

we have the entries of the FRM,

$$g_{11}^I = \lambda_1^2\sum_i r_i^2\cos^2\left(\theta_i - \frac{\beta}{2}\right), \tag{43}$$

$$g_{22}^I = \lambda_2^2\sum_i r_i^2\cos^2\left(\theta_i + \frac{\beta}{2}\right), \tag{44}$$

$$g_{12}^I = \lambda_1\lambda_2\sum_i r_i^2\cos\left(\theta_i + \frac{\beta}{2}\right)\cos\left(\theta_i - \frac{\beta}{2}\right), \tag{45}$$

henceforth, the square of the DDS,

$$\mathcal{D}_D^2 = g_{11}^I g_{22}^I - \left(g_{12}^I\right)^2 \tag{46}$$

$$= \lambda_1^2\lambda_2^2\sin^2\beta\sum_{i>j} r_i^2 r_j^2\sin^2(\theta_j - \theta_i) \tag{47}$$

$$\leqslant \frac{1}{4}\lambda_1^2\lambda_2^2\sin^2\beta. \tag{48}$$

For a loose constraint, the equality (MDDS) is reached by a variety of projective measurements. Specific for $\hat{\boldsymbol{E}}$ with a uniform distribution $r_i^2 = 1/3$ for all i, the equality is reached by measurements with $\sin^2(\theta_i - \theta_j) = 3/4$ for $i \neq j$, e.g., the special solution

$$\{|k_0\rangle, |k_1\rangle, |k_2\rangle\} = \frac{1}{\sqrt{3}}\begin{bmatrix} 1 & 1 & 1 \\ 1 & e^{i2\pi/3} & e^{i4\pi/3} \\ 1 & e^{i4\pi/3} & e^{i2\pi/3} \end{bmatrix} \tag{49}$$

with the phase $\theta_i = 2i\pi/3$ in the orthogonal complete basis $\{|\psi\rangle, |\nabla_1\psi\rangle, |\psi_\perp\rangle\}$, $\langle\psi|\psi_\perp\rangle = \langle\nabla_1\psi|\psi_\perp\rangle = 0$. This completes our proof. ■

Specifically, the vanishing of $|\mathcal{Q}|$ induces the expansion

$$|\psi(\boldsymbol{\theta} + \delta\boldsymbol{\theta})\rangle \approx |\psi(\boldsymbol{\theta})\rangle + (\delta\theta^1\lambda_1 + e^{i\beta}\delta\theta^2\lambda_2)|\nabla_1\psi\rangle. \tag{50}$$

The parameters' shift $\delta\boldsymbol{\theta}$ is encoded in the coefficient of $|\nabla_1\psi\rangle$. In the vertex measurement $\hat{\boldsymbol{E}}^v$, one can only acquire the magnitude $|\delta\theta^1\lambda_1 + e^{i\beta}\delta\theta^2\lambda_2|$, where $\delta\theta^1$ and $\delta\theta^2$ are mixed together. The estimators cannot be built. The MvDDS thus vanishes. However, via the general ternary-outcome measurement $\hat{\boldsymbol{E}}$, the phase and magnitude of the coefficient are simultaneously attainable. A nonzero DDS is thus acquired.

For two-parameter states with a given Berry curvature $\mathcal{B}_{12}$, the minimal square IDQS is a quarter of $\mathcal{B}_{12}^2$. It is the direct result of the nonnegativity of the quantum geometric tensor $\mathcal{Q}$. From this point of view, Eq. (39) indicates that the minimal MDDS for a given Berry curvature is provided by states with the minimal IDQS determined by the Berry curvature.

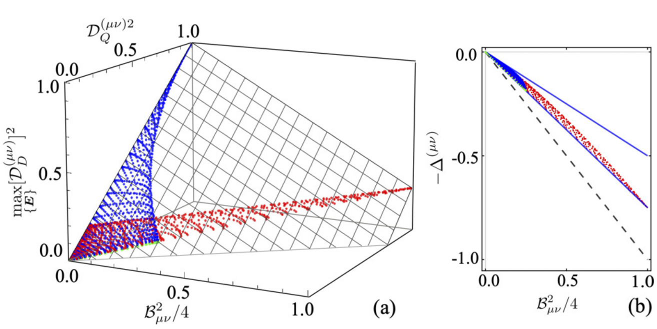

FIG. 4. Codistribution of the IDQS ($\mathcal{D}_Q^{(\mu\nu)}$), MDDS ($\max_{\{\hat{E}\}}[\mathcal{D}_D^{(\mu\nu)}]$), and Berry curvature ($\mathcal{B}_{\mu\nu}$). The MDDS is acquired via numerical optimization. (a) Red, blue, and green dots denote states in the submanifolds $\Theta^{(\alpha\beta)}$, $\Theta^{(\alpha\theta)}$, and $\Theta^{(\gamma\theta)}$, respectively. The plane is given by the equality of Eq. (39). (b) Square gap between the IDQS and the MDDS ($\Delta^{(\mu\nu)}$) vs the Berry curvature ($\mathcal{B}_{\mu\nu}$). The square gap is defined by $\Delta^{(\mu\nu)} = \mathcal{D}_Q^{(\mu\nu)2} - \max_{\{\hat{E}\}}[\mathcal{D}_D^{(\mu\nu)}]^2$.

VI. CONCLUSIONS

In this article, we have studied multiparameter estimation from the information geometry perspective. By taking the FRM as the metric of the statistical manifold, we proposed a measure $\mathcal{D}_D$ called the density of distinguishable states (DDS) with its invariant volume element. The DDS measures the maximal density of states (estimators) distinguishable in the neighborhood of the d-dimensional estimand $\boldsymbol{\theta}$.

The volume of the corresponding estimators $\boldsymbol{\theta}_{\rm est}$ depicts the uncertainty of the multiparameter estimation and is measured by $\sqrt{|4\boldsymbol{\Sigma}|}$, with $\boldsymbol{\Sigma}$ denoting its covariance matrix. As the quantum counterpart of the FRM, the QFM $\boldsymbol{g}^F$ serves as the metric of projective Hilbert spaces. The invariant volume elements of $\boldsymbol{g}^F$ defines the intrinsic density of quantum states (IDQS) $\mathcal{D}_Q$ of the projective Hilbert space. As an application, the IDQS provides us a new method of calculating the (over)completeness relation of a class of states. The examples of coherent states and squeezed states have been given. The ability to infer the IDQS via multiparameter estimation has been studied via the determinant-form quantum Cramér-Rao inequality. As a result, we have found that the IDQS bounds the DDS from above. However, differently from the single-parameter cases, this bound is not exact generally. Exemplified by the three-level system with two parameters, we have shown that the maximal DDS attained via projective measurement is characterized by the Berry curvature. Specifically, the square gap between the IDQS and the maximal DDS attained via vertex measurements equals the square of the Berry curvature. It reveals the inner connections between the gap and the uncertainty principle of quantum theory.

Quantifying the distinguishability of quantum states is one of the central topics in studying the statistical aspects of quantum theory. The QFI and statistical distance perform well in single-parameter cases. As a qualified measure of the distinguishability, the IDQS (DDS) is an essential extension of the statistical distance in multiparameter cases. Their values are promising, as many of the topics we are interested in are generally multiparameter. Theoretically, complex projective Hilbert spaces [36–38], which depict the fundamental geometrical structures of quantum theory, are intrinsically multidimensional. In practical studies such as those of ground-state manifolds [79], the quantum phase transition [80], response theory [82–84], and even thermodynamics [66,77,78,85,86], the systems under investigation are generally multidimensional too. By quantifying the distinguishability of quantum states in these cases, the IDQS (DDS) may provide an impetus for corresponding studies.

Precisely, the IDQS also measures the quantum state's overall response to the small shift of a set of given parameters (of both intrinsic and external control parameters [49–53]). Hence applications of the IDQS to studies such as those on the quantum phase transition [54,55] and dynamics of open quantum systems [59] are promising. The DDS is also an essential measure of multidimensional manifolds in classical information geometry. It is potentially a powerful tool for study of neural networks, classical statistics, and thermodynamics. Furthermore, we have shown that the gap between the IDQS and the maximal DDS is the signature of the uncertainty principle in the framework of information geometry. It confirms the insights that quantum multiparameter estimation is a perfect scenario in which to study the limits of quantum measurements. It further raises some attractive questions such as (i) Do the results for three-level systems hold for general (nonprojective) measurements? and (ii) How does the Berry curvature characterize the gap for higher-dimensional systems? We hope that further studies may reveal more internal connections between multiparameter estimation and quantum measurements.

ACKNOWLEDGMENTS

H.J.X. thanks Yimu Du for the helpful discussion. This work was supported by the National Natural Science Foundation of China (NSFC) (Grants No. 11725417, No. 12088101, and No. U1930403) and the Science Challenge Project (Grant No. TZ2018005).

APPENDIX A: REGULARITY CONDITION OF THE ASYMPTOTIC NORMALITY OF THE LIKELIHOOD ESTIMATORS

We follow the discussion about the asymptotic normality of the roots of likelihood estimation in Sec. 6.5 of [90]. Those conditions indicate that:

(a1) The estimators $\bar{\boldsymbol{\theta}}_{\rm est}(\boldsymbol{\xi})$ are well defined as single-valued functions of $\boldsymbol{\xi}$.

(a2) The FRM $\boldsymbol{g}^I$ is positive definite for all $\boldsymbol{\theta}\in\Theta$, and the entries $\boldsymbol{g}^I_{\mu\nu}$ are finite.

(a3) The third derivatives $\partial_\mu\partial_\nu\partial_\gamma\log[\rho(\boldsymbol{\xi}|\boldsymbol{\theta})]$ exist and are bounded for all $\mu,\ \nu,\ \gamma$, and $\boldsymbol{\theta}\in\Theta$.

Theoretically, one can narrow Θ and the range of estimators to an arbitrary small open subset $\boldsymbol{\omega}$ containing $\boldsymbol{\theta}$ with sufficient prior information. Hence, these conditions can be satisfied by most of the statistical models in quantum metrology. Thus we can assume the existence of asymptotic efficient estimators, i.e., the DDS values are generally attainable.

APPENDIX B: PROOF OF THE COMPLETENESS RELATION, EQ. (14)

We study the $(n+1)$–level system with a set of orthogonal complete basis $\{|0\rangle, |a\rangle | a=1,2,\ldots,n\}$. It spans a Hilbert space $\mathcal{H}$ with the completeness relation

$$|0\rangle\langle 0| + \sum_a |a\rangle\langle a| = \hat{\mathbb{1}}. \tag{B1}$$

An arbitrary pure state in $\mathcal{H}$ can be expanded as

$$|\psi(\boldsymbol{\theta})\rangle = \sum_{a=1}^{n} x_a e^{i\phi_a}|a\rangle + x_0 e^{i\phi_0}|0\rangle, \tag{B2}$$

with $x_0, x_a \geqslant 0$, and the phases $0\leqslant \phi_0, \phi_a < 2\pi$. By further introducing the normality

$$x_0^2 + \sum_a x_a^2 = 1 \tag{B3}$$

and fixing the phase $\phi_0 = 0$, $|\psi(\boldsymbol{\theta})\rangle$ denotes a quantum state in $\mathbb{C}\mathbf{P}^n$ with the real coordinates

$$\boldsymbol{\theta} = (x_1, x_2, \ldots, x_n; \phi_1, \phi_2, \ldots, \phi_n). \tag{B4}$$

Based on the above setups, we show that the IDQS is the measure for constructing the identity (completeness relation) of $\mathcal{H}$, i.e.,

$$\hat{\mathbb{1}} \propto \int d^{2n}\boldsymbol{\theta}\mathcal{D}_Q(\boldsymbol{\theta})|\psi(\boldsymbol{\theta})\rangle\langle\psi(\boldsymbol{\theta})| \equiv \hat{\mathbb{K}}. \tag{B5}$$

We start from the derivative

$$|d\psi(\boldsymbol{\theta})\rangle = \sum_a \partial_a|\psi(\boldsymbol{\theta})\rangle dx_a + \sum_a \partial'_a|\psi(\boldsymbol{\theta})\rangle d\phi_a, \tag{B6}$$

with $\partial_a \equiv \partial/\partial x_a$, $\partial'_a \equiv \partial/\partial \phi_a$, and

$$\partial_a|\psi(\boldsymbol{\theta})\rangle = -x_a/x_0|0\rangle + e^{i\phi_a}|a\rangle, \tag{B7}$$

$$\partial'_a|\psi(\boldsymbol{\theta})\rangle = ix_a e^{i\phi_a}|a\rangle. \tag{B8}$$

Based on it, we have the line element

$$\begin{aligned} ds^2 &= \langle d\psi(\boldsymbol{\theta})|d\psi(\boldsymbol{\theta})\rangle - \langle d\psi(\boldsymbol{\theta})|\psi(\boldsymbol{\theta})\rangle\langle\psi(\boldsymbol{\theta})|d\psi(\boldsymbol{\theta})\rangle \\ &= \sum_{ab}\left(\frac{x_a x_b}{x_0^2} + \delta_{ab}\right)dx_a dx_b \\ &\quad + \sum_{ab}\left(\delta_{ab}x_a^2 - x_a^2 x_b^2\right)d\phi_a d\phi_b. \end{aligned} \tag{B9}$$

This indicates the metric

$$\boldsymbol{g}^F = \begin{bmatrix} (\boldsymbol{g}^F)^{\boldsymbol{x}} & \mathbf{0} \\ \mathbf{0} & (\boldsymbol{g}^F)^{\boldsymbol{\phi}} \end{bmatrix}, \tag{B10}$$

with

$$(\boldsymbol{g}^F)^{\boldsymbol{x}} = \frac{1}{x_0^2}\begin{bmatrix} x_1^2 + x_0^2 & x_1x_2 & \cdots & x_nx_1 \\ x_1x_2 & x_2^2 + x_0^2 & & x_nx_2 \\ \vdots & & \ddots & \vdots \\ x_1x_n & x_2x_n & \cdots & x_n^2 + x_0^2 \end{bmatrix}, \tag{B11}$$

$$(\boldsymbol{g}^F)^{\boldsymbol{\phi}} = \begin{bmatrix} x_1^2 - x_1^4 & -x_1^2x_2^2 & \cdots & -x_n^2x_1^2 \\ -x_1^2x_2^2 & x_2^2 - x_2^4 & & -x_n^2x_2^2 \\ \vdots & & \ddots & \vdots \\ -x_1^2x_n^2 & -x_2^2x_n^2 & \cdots & x_n^2 - x_n^4 \end{bmatrix}. \tag{B12}$$

Hence, we have the IDQS

$$\mathcal{D}_Q(\boldsymbol{\theta}) = \sqrt{|\boldsymbol{g}^F|} = \prod_a x_a. \tag{B13}$$

Inserting it into the right-hand side of Eq. (B5), we have the entries

$$\begin{aligned} \langle c|\hat{\mathbb{K}}|b\rangle &= \int d^n\boldsymbol{x}\mathcal{D}_Q(\boldsymbol{\theta})x_c x_b \int d^n\boldsymbol{\phi} e^{i(\phi_b-\phi_c)} \\ &= \mathrm{Vol}(\mathbb{C}\mathbf{P}^n)/(n+1)\delta_{bc}, \end{aligned} \tag{B14}$$

$$\begin{aligned} \langle 0|\hat{\mathbb{K}}|0\rangle &= \int d^n\boldsymbol{x}\mathcal{D}_Q(\boldsymbol{\theta})x_0^2 \int d^n\boldsymbol{\phi} \\ &= \mathrm{Vol}(\mathbb{C}\mathbf{P}^n)/(n+1), \end{aligned} \tag{B15}$$

$$\begin{aligned} \langle 0|\hat{\mathbb{K}}|b\rangle &= \int d^n\boldsymbol{x}\mathcal{D}_Q(\boldsymbol{\theta})x_0 x_b \int d^n\boldsymbol{\phi} e^{i\phi_b} \\ &= 0, \end{aligned} \tag{B16}$$

with the volume of $\mathbb{C}\mathbf{P}^n$

$$\mathrm{Vol}(\mathbb{C}\mathbf{P}^n) \equiv \int d^{2n}\boldsymbol{\theta}\mathcal{D}_Q(\boldsymbol{\theta}) = \frac{\pi^n}{n!}. \tag{B17}$$

We have thus proved the completeness relation

$$\frac{\pi^n}{(n+1)!}\int d^{2n}\boldsymbol{\theta}\mathcal{D}_Q(\boldsymbol{\theta})|\psi(\boldsymbol{\theta})\rangle\langle\psi(\boldsymbol{\theta})| = \hat{\mathbb{1}}. \tag{B18}$$

Furthermore, we mention that the form of this identity is invariant under re-parameterization, hence its validity is independent of the choice of coordinates.

APPENDIX C: EXAMPLES OF CALCULATING THE COMPLETE RELATIONSHIP WITH THE QFM

1. Coherent states

The coherent states widely used in the quantum optics and quantum information fields are defined as

$$|\alpha\rangle = e^{\alpha\hat{a}^\dagger - \alpha^*\hat{a}}|0\rangle = e^{-|\alpha|^2/2}\sum_{n=0}^{\infty}\frac{\alpha^n}{\sqrt{n!}}|n\rangle, \tag{C1}$$

where $\hat{a}$ ($\hat{a}^\dagger$) denotes a boson annihilation (creation) operator, $|n\rangle = \hat{a}^{\dagger n}|0\rangle/\sqrt{n!}$ is the number state, and α is a complex number. At first, we separate α into two real parameters with $\alpha = R + iI$. The parameter space is $\Theta = \mathbb{R}^2$, which is a two-dimensional submanifold of $\mathbb{C}\mathbf{P}^\infty$. The corresponding derivatives are

$$\partial_R|\alpha\rangle = (\hat{a}^\dagger - R)|\alpha\rangle, \quad \partial_I|\alpha\rangle = (i\hat{a}^\dagger - I)|\alpha\rangle. \tag{C2}$$

We have the entries of the quantum geometric tensor

$$\begin{aligned} \mathcal{Q}_{RI} &= \mathcal{Q}_{IR}^* \\ &= \langle\alpha|\overleftarrow{\partial}_R\partial_I|\alpha\rangle - \langle\alpha|\overleftarrow{\partial}_R|\alpha\rangle\langle\alpha|\partial_I|\alpha\rangle \\ &= i, \end{aligned} \tag{C3}$$

$$\begin{aligned} \mathcal{Q}_{RR} &= \mathcal{Q}_{II} \\ &= \langle\alpha|\overleftarrow{\partial}_R\partial_R|\alpha\rangle - \langle\alpha|\overleftarrow{\partial}_R|\alpha\rangle\langle\alpha|\partial_R|\alpha\rangle \\ &= 1. \end{aligned} \tag{C4}$$

This indicates $\boldsymbol{\mathcal{Q}} = \boldsymbol{g}^F + \mathbf{i}\boldsymbol{\sigma}$ with

$$\boldsymbol{g}^F = \begin{bmatrix} 1 & 0 \\ 0 & 1 \end{bmatrix}, \quad \boldsymbol{\sigma} = \begin{bmatrix} 0 & 1 \\ -1 & 0 \end{bmatrix} \tag{C5}$$

in the coordinates (R, I). Hence we have the integral

$$\begin{aligned} &\int_{\mathbb{R}^2} dRdI\mathcal{D}_Q|\alpha\rangle\langle\alpha| \\ &= \int_{\mathbb{C}} d^2\alpha e^{-|\alpha|^2}\sum_{n,m=0}^{\infty}\frac{\alpha^n\alpha^{*m}}{\sqrt{n!m!}}|n\rangle\langle m| \\ &= 2\pi\sum_{n=0}^{\infty}\int_0^{\infty} d|\alpha|e^{-|\alpha|^2}\frac{|\alpha|^{2n}}{n!}|n\rangle\langle n| \\ &= \pi\sum_{n=0}^{\infty}|n\rangle\langle n|. \end{aligned} \tag{C6}$$

This is the overcompleteness relation of coherent states [98]. We also mention that the metric $\boldsymbol{g}^F$ is Euclidean, which indicates that the manifold composed of coherent states is uniform. This is consistent with the insight that this manifold is formed by the shift of the vacuum states $|0\rangle$ with operator $e^{\alpha\hat{a}^\dagger - \alpha^*\hat{a}}$.

2. Spin-squeezed states

Here, we take the spin-squeezed states or the SU(1,1) coherent states as an example. The states are defined with the SU(1,1) algebra

$$[\hat{K}_1, \hat{K}_2] = -i\hat{K}_0, [\hat{K}_0, \hat{K}_1] = i\hat{K}_0, [\hat{K}_2, \hat{K}_0] = i\hat{K}_1, \tag{C7}$$

with the Casimir operator

$$\hat{C} = \hat{K}_0^2 - \hat{K}_1^2 - \hat{K}_2^2 = \hat{K}_0^2 - \tfrac{1}{2}(\hat{K}_+\hat{K}_- + \hat{K}_-\hat{K}_+). \tag{C8}$$

The basis vector $|k, m\rangle$ of the unitary irreducible representation is defined by

$$\begin{aligned} \hat{C}|k, m\rangle &= k(k-1)|k, m\rangle, \\ \hat{K}_0|k, m\rangle &= (k+m)|k, m\rangle, \end{aligned} \tag{C9}$$

where k is the Bargmann index. The basis vectors $\{|k, m\rangle|m\}$ span the corresponding representation spaces. The completeness relation of this representation is

$$\hat{\mathbb{1}} = \sum_{m=0}^{\infty} |k, m\rangle\langle k, m|. \tag{C10}$$

For single mode-squeezed states, k equals 1/4 (3/4), corresponding to the even (odd) particle number space. For two-mode squeezed states, we have $k = (n_0 + 1)/2$, where n_0 denotes the number difference between the two modes.

The SU(1,1) coherent state is defined as

$$|z, k\rangle = \exp(\zeta\hat{K}_+ - \zeta^*\hat{K}_-)|k, 0\rangle, \tag{C11}$$

with the complex number $z = \zeta/|\zeta| \tanh|\zeta|$ located in an open disk $D = \{z||z| < 1\}$. In the basis $|k, m\rangle$, the SU(1,1) coherent state can be expanded as

$$|z, k\rangle = (1 - |z|^2)^k \sum_{m=0}^{\infty} \sqrt{\frac{\Gamma(2k+m)}{m!\Gamma(2k)}} z^m |k, m\rangle. \tag{C12}$$

Via a detailed calculation, we find that the QFM is

$$\mathbf{g}^F = \frac{k}{2(1 - |z|^2)^2} \begin{bmatrix} 1 & \\ & |z|^2 \end{bmatrix} \tag{C13}$$

in the coordinates $(|z|, \theta)$ with $z = |z|e^{i\theta}$. If $k > 1/2$, we have the integral over the disk D as

$$\begin{aligned} \int_D d|z|d\theta\sqrt{|\mathbf{g}^F|}|z, k\rangle\langle z, k| &= \sum_{m,n=0}^{\infty} \int_0^1 d|z| \int_0^{2\pi} d\theta \frac{k}{2(1-|z|^2)^2}|z|(1-|z|^2)^{2k}\sqrt{\frac{\Gamma(2k+m)\Gamma(2k+n)}{m!\Gamma(2k)\Gamma(2k)n!}} z^m z^{*n}|k, m\rangle\langle k, n| \\ &= \sum_{m=0}^{\infty} \frac{k\pi\Gamma(2k+m)}{m!\Gamma(2k)} \int_0^1 d|z| \frac{|z|^{2m+1}}{(1-|z|^2)^{2-2k}}|k, m\rangle\langle k, m| \qquad \text{(C14)} \\ &= \sum_{m=0}^{\infty} \frac{k\pi\Gamma(2k+m)}{2m!\Gamma(2k)} \frac{\Gamma(2k-1)m!}{\Gamma(2k+m)}|k, m\rangle\langle k, m| \\ &= \frac{k\pi}{2(2k-1)} \sum_{m=0}^{\infty} |k, m\rangle\langle k, m|. \qquad \text{(C15)} \end{aligned}$$

Obviously, this integral is proportional to $\hat{\mathbb{1}}$. Hence we have the identity

$$\hat{\mathbb{1}}^{(k)} = \frac{2(2k-1)}{k\pi} \int_D d\Theta\mathcal{D}_Q(z)|z\rangle\langle z|. \tag{C16}$$

[1] M. Szczykulska, T. Baumgratz, and A. Datta, Multi-parameter quantum metrology, Adv. Phys. X **1**, 621 (2016), and references therein.

[2] J. Liu, H. Yuan, X.-M. Lu, and X. G. Wang, Quantum Fisher information matrix and multiparameter estimation, J. Phys. A: Math. Theor. **53**, 023001 (2020), and references therein.

[3] K. Matsumoto, A new approach to the Cramér-Rao-type bound of the pure-state model, J. Phys. A: Math. Gen. **35**, 3111 (2002).

[4] P. C. Humphreys, M. Barbieri, A. Datta, and I. A. Walmsley, Quantum Enhanced Multiple Phase Estimation, Phys. Rev. Lett. **111**, 070403 (2013).

[5] C. Vaneph, T. Tufarelli, and M. G. Genoni, Quantum estimation of a two-phase spin rotation, Quantum Meas. Quantum Metro. **1**, 12 (2013).

[6] S. Ragy, M. Jarzyna, and R. Demkowicz-Dobrzánski, Compatibility in multiparameter quantum metrology, Phys. Rev. A **94**, 052108 (2016); Erratum: **99**, 029905(E) (2019).

[7] T. Baumgratz and A. Datta, Quantum Enhanced Estimation of a Multidimensional Field, Phys. Rev. Lett. **116**, 030801 (2016).

[8] L. Pezzé, M. A. Ciampini, N. Spagnolo, P. C. Humphreys, A. Datta, I. A. Walmsley, M. Barbieri, F. Sciarrino, and A. Smerzi, Optimal Measurements for Simultaneous Quantum Estimation of Multiple Phases, Phys. Rev. Lett. **119**, 130504 (2017).

[9] M. Gessner, L. Pezzé, and A. Smerzi, Sensitivity Bounds for Multiparameter Quantum Metrology, Phys. Rev. Lett. **121**, 130503 (2018).

[10] J. S. Sidhu, Y. Ouyang, E. T. Campbell, and P. Kok, Tight bounds on the simultaneous estimation of incompatible parameter, arXiv:1912.09218v3.

[11] M. D. Vidrighin, G. Donati, M. G. Genoni, X.-M. Jin, W. S. Kolthammer, M. S. Kim, A. Datta, M. Barbieri, and I. A. Walmsley, Joint estimation of phase and phase diffusion for quantum metrology, Nat. Commun. **5**, 3532 (2014).

[12] P. J. D. Crowley, A. Datta, M. Barbieri, and I. A. Walmsley, Tradeoff in simultaneous quantum-limited phase and loss estimation in interferometry, Phys. Rev. A **89**, 023845 (2014).

[13] P. Kok, J. Dunningham, and J. F. Ralph, Role of entanglement in calibrating optical quantum gyroscopes, Phys. Rev. A **95**, 012326 (2017).

[14] C. W. Helstrom, *Quantum Detection and Estimation Theory* (Academic Press, New York, 1976).
[15] A. S. Holevo, *Probabilistic and Statistical Aspect of Quantum Theory* (North-Holland, Amsterdam, 1982).
[16] V. Giovannetti, S. Lloyd, and L. Maccone, Quantum-enhanced measurements: Beating the standard quantum limit, Science **306**, 1330 (2004).
[17] V. Giovannetti, S. Lloyd, and L. Maccone, Quanutm Metrology, Phys. Rev. Lett. **96**, 010401 (2006).
[18] V. Giovannetti, S. Lloyd, and L. Maccone, Advances in quantum metrology, Nat. Photon. **5**, 222 (2011).
[19] L. Pezzé, A. Smerzi, M. K. Oberthaler, R. Schmied, and P. Treutlein, Quantum metrology with nonclassical states of atomic ensembles, Rev. Mod. Phys. **90**, 035005 (2018), and references therein.
[20] C. L. Degen, F. Reinhard, and P. Cappellaro, Quantum sensing, Rev. Mod. Phys. **89**, 035002 (2017), and references therein.
[21] D. Braun, G. Adesso, F. Benatti, R. Floreanini, U. Marzolino, M. W. Mitchell, and S. Pirandola, Quantum-enhanced measurements without entanglement, Rev. Mod. Phys. **90**, 035006 (2018), and references therein.
[22] R. J. Sewell, M. Koschorreck, M. Napolitano, B. Dubost, N. Behbood, and M. W. Mitchell, Magnetic Sensitivity Beyond the Projection Noise Limit by Spin Squeezing, Phys. Rev. Lett. **109**, 253605 (2012).
[23] C. F. Ockeloen, R. Schmied, M. F. Riedel, and P. Treutlein, Quantum Metrology with a Scanning Probe Atom Interferometer, Phys. Rev. Lett. **111**, 143001 (2013).
[24] W. Muessel, H. Strobel, D. Linnemann, D. B. Hume, and M. K. Oberthaler, Scalable Spin Squeezing for Quantum-Enhanced Magnetometry with Bose-Einstein Condensates, Phys. Rev. Lett. **113**, 103004 (2014).
[25] A. Louchet-Chauvet, J. Appel, J. J. Renema, D. Oblak, N. Kjrgaard, and E. S. Polzik, Entanglement-assisted atomic clock beyond the projection noise limit, New J. Phys. **12**, 065032 (2010).
[26] I. D. Leroux, M. H. Schleier-Smith, and V. Vuletić, Orientation-Dependent Entanglement Lifetime in a Squeezed Atomic Clock, Phys. Rev. Lett. **104**, 250801 (2010).
[27] O. Hosten, N. J. Engelsen, R. Krishnakumar, and M. A. Kasevich, Measurement noise 100 times lower than the quantum-projection limit using entangled atoms, Nature (London) **529**, 505 (2016).
[28] I. Kruse, K. Lange, J. Peise, B. Lücke, L. Pezzé, J. Arlt, W. Ertmer, C. Lisdat, L. Santos, A. Smerzi, and C. Klempt, Improvement of an Atomic Clock Using Squeezed Vacuum, Phys. Rev. Lett. **117**, 143004 (2016).
[29] LIGO Scientific Collaboration, A gravitational wave observatory operating beyond the quantum shot-noise limit, Nat. Phys. **7**, 962 (2011).
[30] LIGO Scientific Collaboration, Enhanced sensitivity of the LIGO gravitational wave detector by using squeezed states of lights, Nat. Photon. **7**, 613 (2013).
[31] C. R. Rao, Information and the accuracy attainable in the estimation of statistical parameters, Bull. Calcutta Math. Soc. **37**, 81 (1945).
[32] S. Amari, *Differential Geometrical Methods in Statistics* (Springer-Verlag, Berlin, 1985).
[33] S. Amari and H. Nagaoka, *Methods of Information Geometry* (Oxford University Press, New York, 2000).
[34] S. Amari, *Information Geometry and Its Applications* (Springer, Tokyo, 2016).
[35] M. V. Berry, The quantum phase, five years after, in *Geometric Phases in Physics*, edited by A. Shapere and F. Wilczek (World Scientific, Singapore, 1989).
[36] I. Bengtsson and K. Zyczkowski, *Geometry of Quantum States* (Cambridge University Press, New York, 2006).
[37] J. Anandan, and Y. Aharonov, Geometry of Quantum Evolution, Phys. Rev. Lett. **65**, 1697 (1990).
[38] D. C. Brody and L. P. Hughston, Geometric quantum mechanics, J. Geom. Phys. **38**, 19 (2001).
[39] W. K. Wootters, Statistical distance and Hilbert space, Phys. Rev. D **23**, 357 (1981).
[40] S. L. Braunstein and C. M. Caves, Statistical Distance and the Geometry of Quantum States, Phys. Rev. Lett. **72**, 3439 (1994).
[41] G. W. Gibbons, Typical states and density matrices, J. Geom. Phys. **8**, 147 (1992).
[42] H.-J. Sommers and K. Życzkowski, Bures volume of the set of mixed quantum states, J. Phys. A: Math. Gen. **36**, 10083 (2003).
[43] J. Dittmann, The scalar curvature of the Bures metric on the space of density matrices, J. Geom. Phys. **31**, 16 (2004).
[44] P. Lévay, The geometry of entanglement: Metrics, connections and the geometric phase, J. Phys. A: Math. Gen. **37**, 1821 (2004).
[45] P. Zanardi, L. Campos Venuti, and P. Giorda, Bures metric over thermal state manifolds and quantum criticality, Phys. Rev. A **76**, 062318 (2007).
[46] M. Hübner, Explicit computation of the Bures distance for density metrics, Phys. Lett. A **163**, 239 (1992).
[47] D. Šafránek, Discontinuities of the quantum Fisher information and the Bures metric, Phys. Rev. A **95**, 052320 (2017).
[48] S. Zhou and L. Jiang, An exact correspondence between the quantum Fisher information and the Bures metric, arXiv:1910.08473v1.
[49] W.-L. You, Y.-W. Li, and S.-J. Gu, Fidelity, dynamic structure factor, and susceptibility in critical phenomena, Phys. Rev. E **76**, 022101 (2007).
[50] S. Yang, S.-J. Gu, C.-P. Sun, and H.-Q. Lin, Fidelity susceptibility and long-range correlation in the Kitaev honeycomb model, Phys. Rev. A **78**, 012304 (2008).
[51] S.-J. Gu, Fidelity susceptibility and quantum adiabatic condition in thermodynamic limits, Phys. Rev. E **79**, 061125 (2009).
[52] S. Garnerone, D. Abasto, S. Haas, and P. Zanardi, Fidelity in topological quantum phases of matter, Phys. Rev. A **79**, 032302 (2009).
[53] S.-J. Gu, Fidelity approach to quantum phase transitions, Int. J. Mod. Phys. B **24**, 4371 (2010).
[54] L. Campos Venuti and P. Zanardi, Quantum Critical Scaling of the Geometric Tensors, Phys. Rev. Lett. **99**, 095701 (2007).
[55] P. Zanardi, P. Giorda, and M. Cozzini, Information-Theoretic Differential Geometry of Quantum Phase Transitions, Phys. Rev. Lett. **99**, 100603 (2007).
[56] A. Dey, S. Mahapatra, P. Roy, and T. Sarkar, Information geometry and quantum phase transitions in the Dicke model, Phys. Rev. E **86**, 031137 (2012).
[57] P. Kumar, S. Mahapatra, P. Phukon, and T. Sarkar, Geodesics in information geometry: Classical and quantum phase transitions, Phys. Rev. E **86**, 051117 (2012).
[58] R. Maity, S. Mahapatra, and T. Sarkar, Information geometry and the renormalization group, Phys. Rev. E **92**, 052101 (2015).

[59] X. M. Lu, X. Wang, and C. P. Sun, Quantum Fisher information flow and non-Markovian processes of open systems, Phys. Rev. A **82**, 042103 (2010).
[60] P. J. Jones and P. Kok, Geometric derivation of the quantum speed limit, Phys. Rev. A **82**, 022107 (2010).
[61] M. Zwierz, Comment on "Geometric derivation of the quantum speed limit," Phys. Rev. A **86**, 016101 (2012).
[62] M. M. Taddei, B. M. Escher, L. Davidovich, and R. L. de Matos Filho, Quantum Speed Limit for Physical Processes, Phys. Rev. Lett. **110**, 050402 (2013).
[63] D. P. Pires, M. Cianciaruso, L. C. Céleri, G. Adesso, and D. O. Soares-Pinto, Generalized Geometric Quantum Speed Limits, Phys. Rev. X **6**, 021031 (2016).
[64] M. Bukov, D. Sels, and A. Polkovnikov, Geometric Speed Limit of Accessible Many-Body State Preparation, Phys. Rev. X **9**, 011034 (2019).
[65] M. Tomka, T. Souza, S. Rosenberg, and A. Polkovnikov, Geodesic paths for quantum many-body systems, arXiv:1606.05890v2.
[66] D. A. Sivak and G. E. Crooks, Thermodynamic Metrics and Optimal Path, Phys. Rev. Lett. **108**, 190602 (2012).
[67] G. M. Rotskoff and G. E. Crooks, Optimal control in nonequilibrium systems: Dynamic Riemannian geometry of the Ising model, Phys. Rev. E **92**, 060102(R) (2015).
[68] P. R. Zulkowski and M. R. DeWeese, Optimal control of overdamped systems, Phys. Rev. E **92**, 032117 (2015).
[69] D. A. Sivak and G. E. Crooks, Thermodynamic geometry of minimum-dissipation driven barrier crossing, Phys. Rev. E **94**, 052106 (2016).
[70] A. Miyake and M. Wadati, Geometric strategy for the optimal quantum search, Phys. Rev. A **64**, 042317 (2001).
[71] C. Cafaro and S. Mancini, An information geometric viewpoint of algorithms in quantum computing, AIP Conf. Proc. **1443**, 374 (2012).
[72] C. Cafaro and S. Mancini, On Grover's search algorithm from a quantum information geometry viewpoint, Phys. A **391**, 1610 (2012).
[73] G. E. Crooks, Measuring Thermodynamic Length, Phys. Rev. Lett. **99**, 100602 (2007).
[74] P. R. Zulkowski, D. A. Sivak, G. E. Crooks, and M. R. DeWeese, Geometry of thermodynamic control, Phys. Rev. E **86**, 041148 (2012).
[75] F. Weinhold, Metric geometry of equilibrium thermodynamics, J. Chem. Phys. **63**, 2479 (1975).
[76] P. Salamon, A. Nitzan, B. Andresen, and R. S. Berry, Minimum entropy production and the optimization of heat engines, Phys. Rev. A **21**, 2115 (1980).
[77] G. Ruppeiner, Thermodynamics: A Riemannian geometric model, Phys. Rev. A **20**, 1608 (1979).
[78] G. Ruppeiner, Riemannian geometry in thermodynamic fluctuation theory, Rev. Mod. Phys. **67**, 605 (1995).
[79] M. Kolodrubetz, V. Gritsev, and A. Polkovnikov, Classifying and measuring geometry of a quantum ground state manifold, Phys. Rev. B **88**, 064304 (2013).
[80] P. Kumar and T. Sarkar, Geometric critical exponents in classical and quantum phase transitions, Phys. Rev. E **90**, 042145 (2014).
[81] L. Banchi, P. Giorda, and P. Zanardi, Quantum information-geometry of dissipative quantum phase transitions, Phys. Rev. E **89**, 022102 (2014).
[82] T. Ozawa, Steady-state Hall response and quantum geometry of driven-dissipative lattices, Phys. Rev. B **97**, 041108(R) (2018).
[83] M. Kolodrubetz, D. Sels, P. Mehta, and A. Polkovnikov, Geometry and non-adiabatic response in quantum and classical systems, Phys. Rep. **697**, 1 (2017).
[84] T. Shitara and M. Ueda, Determining the continuous family of quantum Fisher information from linear-response theory, Phys. Rev. A **94**, 062316 (2016).
[85] D. Brody and N. Rivier, Geometrical aspects of statistical mechanics, Phys. Rev. E **51**, 1006 (1995).
[86] A. Carollo, D. Valenti, and D. Spagnolo, Geometry of quantum phase transitions, Phys. Rep. **838**, 1 (2020).
[87] J. Suzuki, Explicit formula for the Holevo bound for two-parameter qubit-state estimation problem, J. Math. Phys. **57**, 042201 (2016).
[88] R. D. Gill and M. Guta, On asymptotic quantum statistical inference, in *From Probability to Statistics and Back: High-Dimensional Models and Processes* (Institute of Mathematical Statistics, Beachwood, Ohio, 2013), Vol. 9, pp. 105–127.
[89] H. Nagaoka, in *Asymptotic Theory of Quantum Statistical Inference*, edited by M. Hayashi (World Scientific, Singapore, 1989), Vol. 1, Chap. 8.
[90] E. L. Lehmann and G. Casella, *Theory of Point Estimation*, 2nd ed. (Springer-Verlag, New York, 1998), Sec. 6.5.
[91] J. Shao, *Mathematical Statistics*, 2nd ed. (Springer-Verlag, New York, 2003), Sec. 4.5.
[92] H. Jeffreys, An invariant form for the prior probability in estimation problems, Proc. R. Soc. A **186**, 453 (1946).
[93] H. Jeffereys, *Theory of Probability*, 2nd ed. (Oxford University Press, New York, 1948).
[94] E. T. Jaynes, Prior probabilities, IEEE Trans. Syst. Sci. Cybernet. **4**, 227 (1968).
[95] E. T. Jaynes, *Probability Theory: The Logic of Science* (Cambridge University Press, Cambridge, UK, 2003).
[96] R. Hermann, *Lie Groups for Physicists* (Benjamin, New York, 1966).
[97] M. Byrd, Differential geometry on SU(3) with applications to the three state systems, J. Math. Phys. **39**, 6125 (1998).
[98] M. O. Scully and M. S. Zubairy, *Quantum Optics* (Cambridge University, Cambridge, UK, 1997).